The full details of the published version of the article are as follows:

TITLE: Quantitative planar and volumetric cardiac measurements using 64 mdct and 3t mri vs. Standard 2d and m-mode echocardiography: does anesthetic protocol matter?

AUTHORS: Randi Drees, Rebecca A. Johnson, Rebecca L. Stepien, Alejandro Munoz Del Rio, Jimmy H. Saunders and Christopher J. François

JOURNAL TITLE: Veterinary Radiology & Ultrasound

VOLUME/EDITION: 56/6

PUBLISHER: Wiley

PUBLICATION DATE: 16 June 2015 (online)

DOI: 10.1111/vru.12269

Quantitative planar and volumetric cardiac measurements using 64 MDCT and 3T MRI versus standard 2D and M-mode echocardiography: Does anesthetic protocol matter?

Randi Drees[1], Rebecca A Johnson[1], Rebecca L Stepien[2], Alejandro Munoz Del Rio[3,5], Jimmy H Saunders[4], Christopher J François[5]

UW-Madison VMTH [1]DSS and [2]DMS, 2015 Linden Drive, Madison, WI 53706, USA; [3]UW-Madison Department of Medical Physics, 600 Highland Avenue, Madison, WI 53792, USA; [4]UGent, Faculty of Veterinary Medicine, Salisburylaan 133, 9820 Merelbeke, Belgium; [5]UW-Madison, School of Medicine and Public Health, Department of Radiology, 600 Highland Avenue, Madison, WI 53792, USA

Dr. Drees's current address is: Department of Clinical Sciences and Services, The Royal Veterinary College, University of London, Hertfordshire AL9 7TA, UK

Keywords*:*

Dog, computed tomography, magnetic resonance imaging, cardiac function, cardiac size

Running head*:*

CT MRI cardiac measurements

Portions of this study were given as oral presentations for the EVDI conference

2013 in Portugal (volumetric variables) and ACVR conference 2013 in Savannah,

GA, USA (planar variables).

47

48

49

50

51

52 **Abstract**

53 Cross-sectional imaging of the heart utilizing computed tomography (CT) and

54 magnetic resonance imaging (MRI) has been shown to be superior for the

55 evaluation of cardiac morphology and systolic function in humans compared to

56 echocardiography. The purpose of this prospective study was to test the effects of

57 two different anesthetic protocols on cardiac measurements in 10 healthy beagle

58 dogs using 64-multidetector row computed tomographic angiography (64-

59 MDCTA), 3T magnetic resonance (MRI) and standard awake echocardiography.

60 Both anesthetic protocols used propofol for induction and isoflourane for anesthetic

61 maintenance. In addition, protocol A used midazolam/fentanyl and protocol B used

62 dexmedetomedine as premedication and constant rate infusion during the

63 procedure. Significant elevations in systolic and mean blood pressure were

64 present when using protocol B. There was overall good agreement between the

65 variables of cardiac size and systolic function generated from the MDCTA and MRI

66 exams and no significant difference was found when comparing the variables

67 acquired using either anesthetic protocol within each modality. Systolic function

68 variables generated using 64-MDCTA and 3T MRI were only able to predict the

69 left ventricular end diastolic volume as measured during awake echocardiogram

70 when using protocol B and 64-MDCTA. For all other systolic function variables,

71 prediction of awake echocardiographic results was not possible (P = 1). Planar

72 variables acquired using MDCTA or MRI did not allow prediction of the

73 corresponding measurements generated using echocardiography in the awake

74 patients (P=1). Future studies are needed to validate this approach in a more

75 varied population and clinically affected dogs.

76

77 **Introduction**

78 In companion animals the evaluation of cardiac morphology and systolic function

79 has mainly been based on echocardiographic evaluation and cardiac

80 catheterization.[1-6] The potential role of MRI in the future of veterinary clinical

81 cardiology has been reviewed critically[24] and recent publications have utilized MRI

82 and/or MDCT for functional and morphological cardiac evaluations[15, 23, 25-29, 40, 41].

83 Cross-sectional imaging of the heart utilizing computed tomography (CT) and

84 magnetic resonance imaging (MRI) has shown to be superior for the evaluation of

85 cardiac morphology and systolic function in humans compared to

86 echocardiography.[7-14] Apart from case reports describing congenital or neoplastic

87 morphological abnormalities involving the heart or great vessels in companion

88 animals[15-22] these modalities have rarely been compared for their use in evaluation

89 of cardiac function.[23-29] While these cross-sectional exams are generally

90 performed in the awake human patient,[30] companion animal patients require

91 anesthesia or heavy sedation at a minimum to undergo these studies. Although

92 different anesthetic protocols have been used,[23, 25, 27-29, 31] the effects of specific

4

93   anesthetic protocols on image quality, systolic function and cardiac morphologic

94   variables as determined by cross-sectional imaging have not been systematically

95   evaluated. Furthermore, to optimize image quality, a target heart rate of <65bpm

96   is recommended for multidetector computed tomographic angiography (MDCTA)

97   in people.[32]   The canine heart rate varies with many factors, including choice of

98   anesthetic/sedative agents as well as body weight; however, rates between 80-

99   150 are commonly seen in awake patients.[33]

100

101   The primary goal of this study was to analyze variables of cardiac morphology and

102   systolic function using 64 MDCTA and magnetic resonance imaging (MRI) at 3

103   Tesla by comparing two anesthetic protocols for heart rate control and impact on

104   cardiac function in 10 healthy dogs. The secondary goal was to compare the

105   variables of cardiac size and systolic function generated by MDCTA to MRI and to

106   relate those to the current clinical practice of echocardiography in the awake dog.

107   The results were intended to provide baseline recommendations for further cardiac

108   investigations using MDCTA and MRI in dogs. The hypothesis for this study was

109   that parameters acquired using CT and MRI with either anesthetic protocol would

110   be comparable but differ from parameters acquired using echocardiography on the

111   awake dogs.

112

113   **Material and Methods**

114   *Animal preparation:* The University of Wisconsin's Institutional Animal Care and

115   Use Committee approved all procedures. Ten purpose-bred healthy beagle dogs

116   with a mean age of 10.4 (range 7-20) months and mean body weight of 10.7 (range

117   8.9-12.7) kg were used in this study and underwent awake echocardiography once

118   and then retrospectively EKG-gated MDCTA and MRI under anesthesia on two

119   different days, using a different anesthetic protocol for each of the two anesthetic

120   episodes. The order of MDCTA and MRI was randomized as well as the order of

121   the anesthetic protocols for heart rate regulation for each dog.

122   A 20G intravenous catheter was placed in the both the right and left cephalic veins;

123   the left was used for anesthesia purposes and the right for contrast administration

124   in all dogs. Anesthetic monitoring included modality specific recording of

125   electrocardiography (using the footpads for the CT exam and the chest for the MRI

126   exam for electrode placement) as well as pulse-oximetry to monitor heart rate,

127   rhythm and hemoglobin saturation; systolic, diastolic and mean blood pressure

128   was non-invasively monitored with a cardiac monitor (Cardell® Veterinary Monitor,

129   Model 9401, CAS Medical Systems, Branford, CT, 06405). Short periods of apnea

130   were induced by mild hyperventilation and halting the mechanical ventilator when

131   needed during image acquisition.

132   *Echocardiography:* standard awake auscultation and echocardiographic exam

133   (Vivid 7, GE Health Care, Waukashea, WI, USA, 8 and 5MHz transducers) was

134   performed by a board certified veterinary cardiologist (RLS) once, prior to the

135   anesthetic episodes for cross-sectional imaging. The following variables were

136   recorded using M-mode: diastolic and systolic interventricular septal thickness

137   (IVSd, IVSs), left ventricular internal diameter (LVIDd, LIVDs) and left ventricular

138   posterior wall thickness (LVPWd, LVPWs). Additionally standard single plane 2D

139 B-mode images were used to acquire measurements of the aortic, left atrial and

140 main pulmonary arterial diameter; left atrium to aorta ratio (LA/Ao ratio) and aorta

141 to pulmonary artery (Ao/PA ratio) were calculated from those measurements.

142 Fractional shortening (FS %) was calculated using the following formula: FS =

143 (LVIDd – LVIDs)/LVIDd x 100. End diastolic volume (EDV), end systolic volume

144 (ESV), ejection fraction (EF) and stroke volume (SV) were calculated using the

145 Simpson method.[34] Left ventricular mass was calculated from M-mode

146 measurements using the following formula: $LVM = 1.04 \times [(LVIDd + LVWd + IVSd)^3$

147 $– (LVIDd)^3] – 13.6g^2$.

148 *Anesthesia protocols:* All dogs were induced using a propofol bolus to effect (2-6

149 mg/kg) for each of the two cross-sectional imaging events. The animals were orally

150 intubated, placed in dorsal recumbency in a custom made trough for positioning in

151 CT and MRI and maintained on isoflurane (Vaporizer set at 1-2%) and 100%

152 oxygen using mechanical ventilation to an end-tidal CO2 level between 35-

153 40mmHg. The dogs also received maintenance intravenous Lactated Ringer's

154 Solution (5-10 ml/kg/hr; Abbott Laboratories, North Chicago, IL, USA) through the

155 left cephalic catheter. Protocol A used fentanyl (Fentanyl Citrate, West-ward,

156 Eatontown, NJ, USA) 5µg/kg bolus for premedication followed by 10µg/kg/hr

157 continuous rate infusion (CRI) and midazolam (Midazolam, Hospira, Inc., Lake

158 Forest, IL, USA) 0.2mg/kg bolus followed by 0.2mg/kg/hr CRI. Protocol B used

159 dexmedetomedine (Dexdomitor, Pfizer Animal Health, New York, New York, USA)

160 1-2µg/kg bolus for premedication and 1-2µg/kg/hr CRI.

161 *Cardiac MDCTA:* Cardiac exams were performed using a 64-MDCT unit

162 (Discovery CT750 HD, General Electrics Medical Systems, Waukesha, WI, USA).

163 A transverse plane helical exam of the thorax was performed using 1.25mm slice

164 thickness and reconstruction interval, medium frequency reconstruction kernel,

165 80kVp, 200mA, 0.35s tube rotation time and a pitch of 0.51, followed by acquisition

166 of a localizer image over the right ventricular outflow tract and the aortic root. Using

167 the semi-automated bolus tracking function a retrospectively EKG-gated cardiac

168 MDCTA was performed using 15ml iodinated contrast medium (Omnipaque 300,

169 NovaPlus GE Healthcare, Princeton, NJ, USA) followed by a 5ml saline flush

170 administered from a dual barrel injector at 2ml/s and 325PSI. Contrast injection

171 was timed to mainly opacify the left atrium, left ventricle, coronary arteries and

172 thoracic aorta. Scan parameters used for the retrospectively gated scan were set

173 to 1.25mm slice thickness, 0.625mm spacing between slices, medium frequency

174 reconstruction algorithm, DFOV 12cm centered over the heart, 80kVp, 400mA,

175 0.35s tube rotation time and helical pitch of 0.24.

176 *Cardiac MRI:* The exams were performed using a 3 Tesla MRI unit (Discovery

177 MR750, GE Healthcare, Waukesha, WI, USA) using a 32-channel upper torso coil.

178 Insulated EKG leads were placed on the chest wall, as placement of EKG leads

179 on the footpads using non-insulated cables did not produce an EKG trace when

180 the dogs were advanced into the magnet. Localizer scans were acquired in three

181 planes. Then the following sequences were acquired: EKG-gated cine transverse

182 plane, approximate three chamber, approximate four chamber, short axis cine

183 balanced steady-state free precession (SSFP; TR 3.3-4.1ms, TE 45ms, 45 degree

184   flip angle, 224x224 matrix, FOV 230-310x184-207mm, pPOV 0.6-0.8, VPS 12-18,

185   ETL 1, NEX 1, BW 125, 6mm slice thickness).

186   After the last cross-sectional imaging modality per day was completed the animals

187   were recovered; after the last episode the dogs were humanely euthanized

188   according to institutional protocol requirements.

189

190   *Image analysis:* Evaluation of the MDCTA and MRI studies was performed using

191   semi-automated software (OsiriX 5.6 64-bit[35] and ReportCARD™ 4.4.6, GE

192   Healthcare, Waukesha, WI, USA, respectively) by a board certified veterinary

193   radiologist (RD) under guidance of a human radiologist specialized in

194   cardiovascular imaging (CJF). The exams were randomized for evaluation and

195   the reviewer was blinded to the anesthetic protocol used for each study. Short

196   axis, approximate three- and four-chamber views of the MDCTA images were

197   generated at 1.25mm slice thickness using open source software[35] to mirror the

198   plane alignment generated in the MRI exams. All studies were inspected for

199   diagnostic image quality to apply measurements by evaluating for adequate

200   contrast, border definition and presence or absence of artifacts.

201   Using the short axis planes, regions of interest were semi-automatically drawn

202   along the endocardial and epicardial border on all images including the left

203   ventricle from the apex to the level of the annulus; where slices with greater than

204   25% of annulus in the imaging plane marked the basal border of the ventricle

205   included in the evaluation. The papillary muscles were included in the ventricular

206   volume for consistency (Figure 1). Using the transverse plane images, semi-

207 automated regions of interest were also placed along the endocardial borders of

208 the right ventricle, where the tricuspid and pulmonic annulus marked the borders

209 of the ventricular volume included, also here the papillary muscles were included

210 with the ventricular volume for consistency (Figure 2). This method was used to

211 generate the following volumetric variables from the MDCTA and MRI exams

212 respectively using the Simpson method:[36] Left ventricular end diastolic and end

213 systolic volume (LVEDV and LVESV); left ventricular end diastolic and end systolic

214 epicardial volume (epiEDV and epiESV). Left ventricular stroke volume (LVSV =

215 LVEDV - LVESV) and left ventricular ejection fraction (LVEF = LVSV / LVEDV)

216 were calculated from these measurements. To verify alignment of the regions of

217 interest drawn only 10% variability between the measurements for left ventricular

218 end diastolic and end systolic myocardial mass (LVmassD and LVmassS) was

219 allowed per dog within the same and between anesthetic episodes. Right

220 ventricular diastolic volume (RVEDV) and right ventricular end systolic volume

221 (RVESV) were recorded; right ventricular stroke volume (RVSV = RVEDV –

222 RVESV) and right ventricular ejection fraction (RVEF = RVSV / RVESV) were

223 calculated from these measurements.

224 The following planar measurements were obtained: systolic and diastolic

225 interventricular septal wall thickness (IVSs, IVSd) and left ventricular posterior wall

226 thickness (LVPWs, LVPWd) thickness; left ventricular internal diameter (LVIDs,

227 LVIDd), mitral and aortic annulus diameter, proximal aortic, proximal pulmonary

228 artery and left atrial diameter.

229 The short axis view, corresponding to the right parasternal short axis view used in

230 echocardiography, was used to measure the systolic and diastolic interventricular

231 septal wall and left ventricular posterior wall thickness as well as the internal

232 diameter of the left ventricle (Figure 3).

233 Fractional shortening (FS %) was calculated from these values (FS = (LVIDd –

234 LVIDs)/LVIDd x 100).

235 The approximate three chamber view, corresponding to the parasternal long axis

236 view used in echocardiography, was used to measure the end systolic left atrial

237 diameter and aortic annulus diameter just prior to opening of the mitral valves and

238 while the aortic valves were open as well as end diastolic mitral annulus diameter

239 while the mitral valves were open (Figure 4 and 5). The left atrium/aorta ratio

240 (La/Ao ratio) was calculated from these values (La/Ao = left atrial diameter/aortic

241 annulus diameter). The approximate four chamber view, corresponding to the left

242 apical four chamber view as used in echocardiography, was used for a repeat

243 measurement of the mitral annulus (Figure 6). The transverse plane views, similar

244 to the right parasternal short axis views in echocardiography, were used to

245 measure the diameter of the proximal aorta and the main pulmonary artery (Figure

246 7). The aorta/pulmonary artery ratio (Ao/Pa ratio) was calculated from these

247 measurements (Ao/Pa = base of the aorta diameter/main pulmonary artery

248 diameter).

249

250 *Statistical analysis:* Open source software was used for statistical evaluation.[37] For

251 all variables evaluated summary statistics (quartiles, mean, standard deviation

252   (SD), minimum and maximum) were computed by one observer (AMR). Medians

253   and extremes were recorded.

254   To establish baseline comparison of the two anesthetic protocols within each

255   imaging modality (i.e. MDCTA and MRI) the data was compared with a paired

256   Wilcoxon signed rank test. Significance was set at P ≤ 0.05. One test was done for

257   MDCTA values and another for the MRI values. Within each type of measurement

258   (i.e. individual variables to compare) the P-values were adjusted with a Holm-

259   Bonferroni step-down procedure.[38]

260   To characterize the typical discrepancy between MDCTA and MRI when

261   measuring the same cardiac attribute, Bland-Altman 95% limits of agreement

262   analysis was used; bias (average difference), lower (LLOA) and upper level of

263   agreement (ULOA) are reported. As both anesthesia protocols were pooled,

264   possible correlation arising from the repeated measures needed to be allowed for,

265   since each dog contributed two observations.[39]

266   Lastly, the results for the left ventricular systolic function and planar variables

267   generated using the cross-sectional modalities with each anesthetic protocol were

268   compared to the comparable variables acquired using echocardiography using the

269   Friedman rank sum test, pairwise comparisons were then generated using the

270   Wilcoxon signed rank test. A simple linear regression was used to determine

271   whether any of the anesthesia-by-imaging modality combinations could predict the

272   values observed with echocardiography when the dogs were awake. The Holm-

273   Bonferroni step-down procedure was used to adjust the P-values for the

274   significance of the slope variable.[38]

275

Results

277 On awake auscultation, 2/10 dogs had an irregular cardiac rhythm and no murmurs

278 were auscultated in any dog at an average heart rate of 115 ± 19bpm. One dog

279 had a marked respiratory sinus arrhythmia during echocardiography; the

280 remaining 9 dogs had a normal sinus rhythm. Echocardiographic examination

281 showed a trivial amount of mitral regurgitation in one dogs and trace tricuspid

282 insufficiency in one dog. Two dogs showed very mild left ventricular enlargement

283 with normal function. Overall, no hemodynamically significant abnormalities were

284 noted in any of the 10 dogs.

285 Both anesthetic protocols provided adequate anesthesia of all dogs and recovery

286 was uneventful in all cases. The median (minimum-maximum) heart rate with

287 protocol A was 81.6 (68.6-96.0) bpm and 76.8 (66-98.6) bpm (P = 1) during the

288 MDCTA and MRI exam respectively. Using protocol B, the median heart rate was

289 73.3 (62.7-102.6) bpm and 71 (64.4-118.8) bpm (P = 1) during the MDCTA and

290 MRI exam, respectively. In one dog the target heart rate of < 65bpm was

291 consistently achieved using protocol B. Vital variables recorded during the CT and

292 MRI exams using protocol A and B are summarized in detail in Table 1. Comparing

293 protocol A and B, diastolic and mean blood pressure were significantly higher (P =

294 0.033 and P = 0.012) and systolic blood pressure was marginally higher (P = 0.052)

295 using protocol B. There was no significant difference found between the remaining

296 recorded physiological values using either protocol (systolic blood pressure P =

297 0.052, Co2 P = 0.075; Table 1). One dog experienced slight tachycardia

13

298   immediately following CT contrast medium administration but the heart rate

299   spontaneously returned to pre-contrast levels within 10 minutes of administration.

300   On average the duration of the MDCTA exam including set up of the dogs,

301   acquisition of localizer images, pre contrast exam and retrospectively gated

302   cardiac exam was 9.31 ± 0.17min; the duration of the retrospectively gated

303   angiography itself lasted an average of 5.0 ± 0.68s. Average duration of the MRI

304   exam including patient positioning, setup of anesthetic and gating equipment,

305   acquisition of localizer images and the cardiac exam lasted for 51.0 ± 3.26min. In

306   the first study dog, delays were encountered, mainly due to difficulties in obtaining

307   an accurate EKG signal, which was remedied by switching to a different, insulated,

308   EKG cable. Thus, this time was not accounted for in calculation of the average

309   duration. The acquisition of the four plane SFFP sequences only took 19.21 ±

310   7.58min.

311   The smart prep feature was used to manually trigger the angiographic exam when

312   contrast medium was seen in the right ventricular outflow tract; the MDCT unit had

313   an inherent additional delay of 5s to start the diagnostic scan. All MDCTA and MRI

314   exams resulted in studies of diagnostic image quality. Mild motion artifact was seen

315   on the MDCTA studies during systole but did not influence the ability to apply

316   measurements. This was mainly displayed as a mild shift between the acquisition

317   segments during systole.

318   Volumetric measurements generated from the awake echocardiograms, MDCTA

319   and cardiac MRI using anesthetic Protocol A and B are listed in Table 2. There

320   were no significant differences for the evaluated volumetric variables between

14

321   the two anesthetic protocols when comparing within the individual cross-sectional

322   modalities (MDCTA and MRI, $P > 0.05$; Table 2 and 3). Comparing the evaluated

323   planar variables between the two anesthetic protocols within the individual cross-

324   sectional modalities (MDCTA and MRI) using the paired Wilcoxon signed rank

325   test, no significant differences were found for any of the variables; $P = 0.292$ for

326   LVIDs using MRI and $P = 1$ for all other variables (Table 3). There was also no

327   difference between the measurements repeated for the same variable on

328   different imaging planes ($P = 1$). The anesthesia protocols were therefore

329   combined for the following analysis. Evaluation of the difference for the

330   volumetric variables generated from MDCTA and MRI while combining the

331   measures for the two different anesthetic episodes per modality and individual as

332   generated by the Bland-Altman analysis are given in Table 4. The graphical

333   output is displayed in Figure 8 for the left ventricular variables and Figure 9 for

334   the right ventricular variables. The bias resulting from the comparison between

335   MDCTA and MRI when accounting for both measures of each individual per

336   modality generated in the Bland-Altman analysis is given in Table 5; Figures 10

337   and 11 show the left ventricular variables and selected further planar

338   measurements respectively as graphical output. Finally, when determining if the

339   left ventricular volumetric values generated using the cross-sectional modalities

340   with anesthetic protocol A and B would be able to predict the comparable

341   variables generated with echocardiography on the awake dog, significant

342   agreement was found only for LVEDV using MDCTA and anesthetic protocol B

343   ($P = 0.01$). All other modality and anesthesia combinations for LVEDV, LVESV,

344 LVSV, LVEF did not agree (P > 0.05) and would not allow for prediction of

345 measurements generated using echocardiography in the awake animal (Table 2,

346 Figure 12).

347 Comparison of the planar variables from the five exams (awake echocardiography

348 and MDCTA, MRI using Protocol A, B) showed significant differences for the

349 following variables: IVSs P=0.0006, LVIDd P=0.03, LVIDs P=0.002, FS P=0.0005,

350 AoDiam P=0.004, LADiam P=0.003, PADiam P=0.0009, LAAoRatio P=0.0421,

351 AoPARatio P=0.048 (Figure 13 and 14). When testing if the planar measurements

352 acquired using the cross-sectional imaging modalities with the dogs anesthetized

353 would be able to predict measurements generated by echocardiography in the

354 awake dog, no significant agreement was found (P = 1 all variables).

355

356

357 **Discussion:**

358 In the current study, diagnostic quality cardiac examinations were successfully

359 acquired in a group of healthy beagle dogs using two different anesthetic protocols

360 and both 64-MDCTA and 3T MRI. The use of different anesthetic protocols for the

361 use in cardiac cross-sectional exams has not yet been evaluated; both anesthetic

362 protocols used in this study were well tolerated and produced comparable results

363 for the vital variables recorded in the healthy study population.

364 Heart rate control has been reported essential for image quality for MDCT

365 acquisitions; high and irregular heart rates will cause motion artifact as the

366 anatomy of the heart and the intravascular bolus may be depicted at different

367 points of the cardiac cycle in the different acquisition segments.[32] The target heart

368 rate of <65 bpm recommended in the human literature for cardiac MDCTA was not

369 reached consistently using either protocol. Despite this, overall very good image

370 quality was achieved at the given temporal resolution using a 64-MDCTA unit and

371 a 0.35s tube rotation time. Mild motion artifact was seen in during systole exams

372 that was displayed as mild shifting between the acquisition segments, yet this did

373 not negatively influence the diagnostic quality of the studies and allowed for all

374 measurements. Further advancement of CT technology using 320 detector row or

375 dual source units are further increasing the speed of image acquisition and may

376 lessen the need for lowering the heart rate for cardiac CT exams in the future.[57] A

377 recent study used dual source MDCT for the evaluation of left ventricular volumes

378 in dogs, and even though no specific comments on image quality were made a

379 mean heart rate greater than 70 bpm allowed for acquisition of the volumetric

380 measurements.[29]

381 The SSFP MRI sequences were acquired retrospectively EKG-gated during a

382 breath hold. The arrhythmia rejection feature was turned off during acquisition as

383 this commonly aborted the scan on the initial dog. The time to repetition (TR) is a

384 function of the patients heart rate as recorded by the gating software and varied

385 between 3.3-4.1ms in the exams and resulted in excellent image quality at the

386 given heart rates.[58]

387 Left ventricular systolic function variables investigated in this study were LVEDV,

388 LVESV, LSV, LVEF and no difference between either anesthetic protocol or either

389 of the three imaging modalities was identified. This differs from a recent study

390   using a similar population of dogs, where the authors report higher end diastolic

391   volume values generated on cardiac CT exams compared to MRI exams

392   represented by a linear relationship between the modalities.[28] The reason for this

393   disagreement is not clear but we speculate that this might relate to a systematic

394   discrepancy in the evaluation of the measurements performed between CT or MRI

395   versus a true alteration induced by the larger contrast bolus injected for the CT

396   exam compared to no contrast injected for the MRI exam; alternatively the order

397   of imaging modalities was not randomized in that study and an effect of anesthetic

398   duration may have contributed. It is important to verify inclusion of the same portion

399   of the heart in the analysis by comparison of the systolic to diastolic myocardial

400   volume mass as calculated by subtraction of endocardial from the epicardial

401   volumes; this was performed in our study and might have aided to minimize an

402   effect by modality compared to the report by Sieslack et al.[28]

403   In addition, since all dogs also had a low level (~1-2%) of isoflurane added to their

404   anesthetic protocol in our study, any potential differences in these variables

405   associated with the two protocols may have been masked by isoflurane since

406   administration produces dose-dependent cardiovascular depression in dogs.[59]

407   Measurement of the myocardial mass is of interest in people in evaluating

408   hypertrophic cardiomyopathies or the effects of downstream hypertension and is

409   used as an independent variable in patients with heart disease. It has also been

410   applied in experimental animal studies for the left and right ventricle.[2, 60-63] This

411   variable has rarely been reported generated using MRI or MDCTA in companion

412   animals   but   left   myocardial   wall   thickness   is   regularly   included   in

413 echocardiographic reporting in companion animals and further evaluation of this

414 variable might be helpful in companion animal cardiac MRI or MDCTA.[26, 31, 64, 65]

415 Inclusion or exclusion of the papillary muscles into the ventricular volume has been

416 used variably between authors and exclusion of the papillary muscles from the left

417 ventricular volume will naturally result in small systematic differences in the

418 quantitative values.[60, 62, 66, 67] In echocardiographic exams the papillary muscles

419 are typically disregarded using Simpson's rule estimates and by definition in

420 Teichholz estimates.[68] Automated threshold based 3D segmentation methods can

421 be used to assess ventricular function and will usually exclude the papillary

422 muscles from the ventricular lumen as the attenuation of intraluminal contrast

423 medium versus the myocardium is used for threshold settings.[66]

424 We aimed to keep the contrast and saline chaser volume low in the MDCT part of

425 our study to avoid volume overloading of the dogs; ventricular contrast achieved

426 was adequate to depict the anatomy to semi-automatically outline the endocardial

427 surfaces of the left and, despite the relatively small contrast volume used, also the

428 right ventricle. However the ventricular enhancement was at the low end for

429 recognition using automated threshold settings so these could not be consistently

430 applied and planar measurements (Simpson method) were therefore performed in

431 this study using the short axis planes for the left and transverse planes for the right

432 heart. This is more time consuming for the evaluator and bears potential room for

433 observer variance; this study used one evaluator to avoid introduction of inter-

434 observer variation. The papillary muscles were consistently included in the

435 ventricular volume in our study due to institutional preference. Overall the LVEDV

436   reported in our study is slightly lower as reported by Sieslack[28] whereas the stroke

437   volumes reported are fairly similar. This may therefore relate to the inclusion of the

438   papillary muscles but a difference caused by the anesthetic protocols used cannot

439   be ruled out since they affect the cardiovascular system to differing degrees.

440   Systolic right ventricular function variables have not been investigated in

441   companion animals using cross-sectional modalities but this gains progressive

442   interest for evaluation in people.[60, 69] This study showed also no difference

443   between the two anesthetic protocols as well as imaging modality used for the

444   assessment of RVEDV, RVESV, RVSV and RVEF and delivers an initial reference.

445   Overall, no difference was found for any of the evaluated planar variables using

446   either anesthetic protocol within the modalities, MDCTA or MRI. This would make

447   the use of the protocols interchangeable for evaluation of these variables within

448   each modality. There was also a low bias in comparing MDCTA and MRI for all

449   variables when the anesthesia protocols were combined. However, because our

450   study was performed in healthy dogs, we cannot extrapolate our data to other

451   species or to patients with cardiovascular diseases or abnormalities.

452   Placement of the measurements was overall easily performed, only over the

453   caudal aspect of the left atrium mild flow-artifact from the pulmonary venous inflow

454   made the delineation of the caudal atrial border difficult at times. However, the bias

455   between the measurements acquired on MDCTA and MRI was only 0.3cm for this

456   variable; though this should be considered as a possible disadvantage when using

457   MRI to evaluate the caudal left atrial border.

458   As expected, the MRI and CT variables acquired using anesthesia protocols A and

459   B produced different values to those acquired in the awake animals using

460   echocardiography. Left end diastolic volumes were higher, end systolic volumes

461   were lower; left ventricular stroke volume and ejection fractions were higher using

462   echocardiography in the awake animals compared to any of the anesthesia

463   modality combinations, even though there was overlap. These findings are

464   consistent with those found in previous studies in isoflurane-anesthetized dogs.[70]

465   A recent study compared echocardiographic measurement of the left ventricular

466   volume using the Teicholz and modified Simpson method to left ventricular

467   volumes acquired using dual source CT and applying the Simpson method in

468   seven propofol/isoflourane anesthetized dogs using medetomedine as

469   premedication. In this study the left ventricular volumes using the modified

470   Simpson method in echocardiography underestimated the volume both compared

471   to echocardiographic measurement using the Teichholz method and

472   measurements from the dual source CT studies using the modified Simpson

473   method[29]. In a different study using ten propofol/isoflourane anesthetized dogs

474   induced with diazepam and levomethadone showed a high correlation of the mean

475   values for EDV and ESV measured from MDCT or echocardiographic exams,

476   using the Simpson method as preferred calculation of the volumes.[23, 27] Another

477   study evaluated ten dogs using a non-specified anesthetic protocol for assessment

478   of left ventricular volumes using three-dimensional echocardiography and

479   magnetic resonance imaging did not find significant differences for EDV, ESV, and

480 EF between the two modalities, but differences were found comparing to one or

481 two dimensional echocardiographic measurements.[27]

482 The IVSs measurement was larger when evaluated using echocardiography in the

483 awake dogs, possibly indicating higher contractility in the awake compared to

484 anesthetized dog as shown previous reports in isoflurane-anesthetized dogs;[70] this

485 effect was present but weaker for LVPWs. Similarly, the fractional shortening was

486 greater and LVIDs was lower in the awake dogs compared to either of our

487 anesthesia protocols, most likely due to the background of isoflurane in all dogs.[70]

488 The aortic and pulmonary artery diameter was larger in the awake versus

489 anesthetized patients. Although previous reports have reported smaller aortic and

490 pulmonic diameters in isoflurane-anesthetized dogs,[41, 71] others have shown no

491 change.[70] Even though blood pressure measurements were not acquired on the

492 awake dogs, a reduction in systemic and pulmonary diameter is consistent with

493 lower blood pressures associated with isoflurane anesthesia even though a

494 modality specific alteration of acquisition of the variable cannot be fully ruled out.

495 The left atrial diameter was lower evaluated in the awake dogs compared to any

496 of the anesthesia protocol–modality combinations. Mildly reduced cardiac

497 contractility in the anesthetized dogs might explain this finding. Based on the

498 difference in these measurements the LAAo ratio was additionally altered in the

499 anesthetized animals; for the AoPA ratio there was greater overlap but also no

500 predictive value for echocardiography was generated.

501 A previous study used seven isoflourane anesthetized normal beagles to compare

502 anatomical measurements acquired using dual source CT to echocardiographic

503   measurements and found overall good agreement except for the values of the

504   interventricular wall and left ventricular posterior wall thickness in end diastole.[41]

505   The authors of this study speculate that interference of anatomical structures such

506   as the papillary muscles or chorda tendinae in combination with lower far-field

507   image quality in echocardiography compared to the high quality of the dual source

508   CT images may be causative for this discrepancy. As clinical patients are unlikely

509   to undergo an anesthetized echocardiogram before cross-sectional imaging a

510   possible discrepancy of the values as described in our study may be considered.

511   Alternatively evaluation of the cross-sectional measurements in the anesthetized

512   animal compared to awake echocardiography in a larger patient group may show

513   trends that may allow for prediction between the modalities in the future.

514

515   The main limitation of this study includes the low number of study subjects used;

516   ideally a larger and more varied study population representing different dog

517   breeds, sizes and chest morphologies might have been included. MRI studies took

518   markedly longer to acquire than the MDCTA studies; availability of the respective

519   modalities as well as the study question may determine the choice of modality for

520   companion animal patients in the future, as a low bias was present between the

521   modalities in our study. Both modalities resulted in overall very good and

522   diagnostic image quality.

523

524

525

526

527

528

529

530

531

532

533

534

535

536

537

538

539

540

541 References

542 1. Thomas W. Two-dimensional, real-time echocardiography in the dog.
543 *Veterinary Radiology* 1984;**25**: 50-64.
544 2. Stepien RL, Hinchcliff KW, Constable PD, Olson J. Effect of endurance
545 training on cardiac morphology in Alaskan sled dogs. *J Appl Physiol (1985).*
546 1998;**85**: 1368-1375.
547 3. Cornell CC, Kittleson MD, Della Torre P, Haggstrom J, Lombard CW,
548 Pedersen HD, et al. Allometric scaling of M-mode cardiac measurements in normal
549 adult dogs. *Journal of veterinary internal medicine / American College of Veterinary*
550 *Internal Medicine.* 2004;**18**: 311-321.
551 4. Buchanan JW. Selective angiography and angiocardiography in dogs with
552 acquired cardiovascular disease. *Veterinary Radiology.* 1965;**6**: 5-20.
553 5. Buchanan JW, Patterson D.F. Selective Angography and
554 Angiocardiography in Dogs with Congenital Cardiovascular disease. *Veterinary*
555 *Radiology.* 1965;**6**: 21-39.

556	6.	Chetboul V. Advanced techniques in echocardiography in small animals.
557	*Vet Clin North Am Small Anim Pract*. 2010;**40**: 529-543.
558	7.	Asferg C, Usinger L, Kristensen TS, Abdulla J. Accuracy of multi-slice
559	computed tomography for measurement of left ventricular ejection fraction
560	compared with cardiac magnetic resonance imaging and two-dimensional
561	transthoracic echocardiography: a systematic review and meta-analysis. *Eur J*
562	*Radiol*. 2012;**81**: e757-762.
563	8.	Nasis A, Mottram PM, Cameron JD, Seneviratne SK. Current and evolving
564	clinical applications of multidetector cardiac CT in assessment of structural heart
565	disease. *Radiology*. 2013;**267**: 11-25.
566	9.	Peters J, Lessick J, Kneser R, Wachter I, Vembar M, Ecabert O, et al.
567	Accurate segmentation of the left ventricle in computed tomography images for
568	local wall thickness assessment. *Med Image Comput Comput Assist Interv*.
569	2010;**13**: 400-408.
570	10.	Tsang W, Bateman MG, Weinert L, Pellegrini G, Mor-Avi V, Sugeng L, et
571	al. Accuracy of aortic annular measurements obtained from three-dimensional
572	echocardiography, CT and MRI: human in vitro and in vivo studies. *Heart*. 2012;**98**:
573	1146-1152.
574	11.	Alberti JF, de Diego JJ, Delgado RV, Riera JC, Torres RA. [State of the art:
575	new developments in cardiac imaging]. *Rev Esp Cardiol (Engl Ed)*. 2012;**65 Suppl**
576	**1**: 24-34.
577	12.	Achenbach S, Barkhausen J, Beer M, Beerbaum P, Dill T, Eichhorn J, et al.
578	[Consensus recommendations of the German Radiology Society (DRG), the
579	German Cardiac Society (DGK) and the German Society for Pediatric Cardiology
580	(DGPK) on the use of cardiac imaging with computed tomography and magnetic
581	resonance imaging]. *Rofo*. 2012;**184**: 345-368.
582	13.	Al-Mohaissen MA, Kazmi MH, Chan KL, Chow BJ. Validation of Two-
583	Dimensional Methods for Left Atrial Volume Measurement: A Comparison of
584	Echocardiography with Cardiac Computed Tomography. *Echocardiography*. 2013.
585	14.	Coon PD, Pollard H, Furlong K, Lang RM, Mor-Avi V. Quantification of left
586	ventricular size and function using contrast-enhanced real-time 3D imaging with
587	power modulation: comparison with cardiac MRI. *Ultrasound Med Biol*. 2012;**38**:
588	1853-1858.
589	15.	Mai W, Weisse C, Sleeper MM. Cardiac magnetic resonance imaging in
590	normal dogs and two dogs with heart base tumor. *Veterinary radiology &*
591	*ultrasound : the official journal of the American College of Veterinary Radiology*
592	*and the International Veterinary Radiology Association*. 2010;**51**: 428-435.
593	16.	Petite AF, Kirberger RM. Mediastinum. In: Schwarz T, Saunders J (eds):
594	*Veterinary Computed Tomography*. Chichester: Wiley-Blackwell, 2011;249-260.
595	17.	Henninger W. Use of computed tomography in the diseased feline thorax.
596	*The Journal of small animal practice*. 2003;**44**: 56-64.
597	18.	Reetz JA, Buza EL, Krick EL. CT features of pleural masses and nodules.
598	*Veterinary radiology & ultrasound : the official journal of the American College of*
599	*Veterinary Radiology and the International Veterinary Radiology Association*.
600	2012;**53**: 121-127.

601 19.   Marolf AJ, Gibbons DS, Podell BK, Park RD. Computed tomographic
602 appearance of primary lung tumors in dogs. *Veterinary radiology & ultrasound : the*
603 *official journal of the American College of Veterinary Radiology and the*
604 *International Veterinary Radiology Association.* 2011;**52**: 168-172.
605 20.   Prather AB, Berry CR, Thrall DE. Use of radiography in combination with
606 computed tomography for the assessment of noncardiac thoracic disease in the
607 dog and cat. *Veterinary radiology & ultrasound : the official journal of the American*
608 *College of Veterinary Radiology and the International Veterinary Radiology*
609 *Association.* 2005;**46**: 114-121.
610 21.   Armbrust LJ, Biller DS, Bamford A, Chun R, Garrett LD, Sanderson MW.
611 Comparison of three-view thoracic radiography and computed tomography for
612 detection of pulmonary nodules in dogs with neoplasia. *Journal of the American*
613 *Veterinary Medical Association.* 2012;**240**: 1088-1094.
614 22.   Schuller S, Fredericksen M, Schroder H, Meyer-Lindenberg A, Hewicker-
615 Trautwein M, Nolte I. [Computer tomographic differentiation of intrathoracic
616 neoplasms and inflammation in the dog]. *Berl Munch Tierarztl Wochenschr.*
617 2005;**118**: 76-84.
618 23.   Henjes CR, Hungerbuhler S, Bojarski IB, Nolte I, Wefstaedt P. Comparison
619 of multi-detector row computed tomography with echocardiography for
620 assessment of left ventricular function in healthy dogs. *American journal of*
621 *veterinary research.* 2012;**73**: 393-403.
622 24.   Gilbert SH, McConnell FJ, Holden AV, Sivananthan MU, Dukes-McEwan J.
623 The potential role of MRI in veterinary clinical cardiology. *Vet J.* 2010;**183**: 124-
624 134.
625 25.   Contreras S, Vazquez JM, Miguel AD, Morales M, Gil F, Lopez O, et al.
626 Magnetic resonance angiography of the normal canine heart and associated blood
627 vessels. *Vet J.* 2008;**178**: 130-132.
628 26.   MacDonald KA, Kittleson MD, Garcia-Nolen T, Larson RF, Wisner ER.
629 Tissue Doppler imaging and gradient echo cardiac magnetic resonance imaging
630 in normal cats and cats with hypertrophic cardiomyopathy. *Journal of veterinary*
631 *internal medicine / American College of Veterinary Internal Medicine.* 2006;**20**:
632 627-634.
633 27.   Meyer J, Wefstaedt P, Dziallas P, Beyerbach M, Nolte I, Hungerbuhler SO.
634 Assessment of left ventricular volumes by use of one-, two-, and three-dimensional
635 echocardiography versus magnetic resonance imaging in healthy dogs. *American*
636 *journal of veterinary research.* 2013;**74**: 1223-1230.
637 28.   Sieslack AK, Dziallas P, Nolte I, Wefstaedt P. Comparative assessment of
638 left ventricular function variables determined via cardiac computed tomography
639 and cardiac magnetic resonance imaging in dogs. *American journal of veterinary*
640 *research.* 2013;**74**: 990-998.
641 29.   Lee M, Park N, Lee S, Lee A, Jung J, Kim Y, et al. Comparison of
642 echocardiography with dual-source computed tomography for assessment of left
643 ventricular volume in healthy Beagles. *American journal of veterinary research.*
644 2013;**74**: 62-69.

645 30.   Mahabadi AA, Achenbach S, Burgstahler C, Dill T, Fischbach R, Knez A, et
646 al. Safety, efficacy, and indications of beta-adrenergic receptor blockade to reduce
647 heart rate prior to coronary CT angiography. *Radiology*. 2010;**257**: 614-623.
648 31.   McDonald KM, D'Aloia A, Parrish T, Mock J, Hauer K, Stillman AE, et al.
649 Functional impact of an increase in ventricular mass after myocardial damage and
650 its attenuation by converting enzyme inhibition. *J Card Fail*. 1998;**4**: 203-212.
651 32.   Menke J, Unterberg-Buchwald C, Staab W, Sohns JM, Seif Amir Hosseini
652 A, Schwarz A. Head-to-head comparison of prospectively triggered vs
653 retrospectively gated coronary computed tomography angiography: Meta-analysis
654 of diagnostic accuracy, image quality, and radiation dose. *Am Heart J*. 2013;**165**:
655 154-163 e153.
656 33.   Hezzell MJ, Dennis SG, Humm K, Agee L, Boswood A. Relationships
657 between heart rate and age, bodyweight and breed in 10,849 dogs. *The Journal
658 of small animal practice*. 2013;**54**: 318-324.
659 34.   Wess G MJ, Simak J, Hartman K. Use of Simpson's Method of Disc to
660 Detect Early Echocardiographic Changes in Doberman Pinschers with Dilated
661 Cardiomyopathy. *Journal of Veterinary Internal mMedicine*. 2010;**24**: 1069-1076.
662 35.   Rosset A, Spadola L, Ratib O. OsiriX: an open-source software for
663 navigating in multidimensional DICOM images. *J Digit Imaging*. 2004;**17**: 205-216.
664 36.   Hergan K, Schuster A, Fruhwald J, Mair M, Burger R, Topker M.
665 Comparison of left and right ventricular volume measurement using the Simpson's
666 method and the area length method. *Eur J Radiol*. 2008;**65**: 270-278.
667 37.   R Development Core Team. *R: A language and environment for statistical
668 computing.* . Vienna: R Foundation for Statistical Computing, 2012.
669 38.   Holm S. A simple sequentially rejective multiple test procedure.
670 *Scandinavian Journal of Statistics*. 1979;**17**: 571-582.
671 39.   Bland JM, Altman DG. Agreement between methods of measurement with
672 multiple observations per individual. *J Biopharm Stat*. 2007;**17**: 571-582.
673 40.   Hockings PD, Busza AL, Byrne J, Patel B, Smart SC, Reid DG, et al.
674 Validation of MRI measurement of cardiac output in the dog: the effects of
675 dobutamine and minoxidil. *Toxicol Mech Methods*. 2003;**13**: 39-43.
676 41.   Park N, Lee M, Lee A, Lee S, Song S, Jung J, et al. Comparative study of
677 cardiac anatomic measurements obtained by echocardiography and dual-source
678 computed tomography. *J Vet Med Sci*. 2012;**74**: 1597-1602.
679 42.   Pascoe PJ, Raekallio M, Kuusela E, McKusick B, Granholm M. Changes in
680 the minimum alveolar concentration of isoflurane and some cardiopulmonary
681 measurements during three continuous infusion rates of dexmedetomidine in
682 dogs. *Vet Anaesth Analg*. 2006;**33**: 97-103.
683 43.   Braz LG, Braz JR, Castiglia YM, Vianna PT, Vane LA, Modolo NS, et al.
684 Dexmedetomidine alters the cardiovascular response during infra-renal aortic
685 cross-clamping in sevoflurane-anesthetized dogs. *J Invest Surg*. 2008;**21**: 360-
686 368.
687 44.   Lin GY, Robben JH, Murrell JC, Aspegren J, McKusick BC, Hellebrekers
688 LJ. Dexmedetomidine constant rate infusion for 24 hours during and after propofol
689 or isoflurane anaesthesia in dogs. *Vet Anaesth Analg*. 2008;**35**: 141-153.

690   45.   Uilenreef JJ, Murrell JC, McKusick BC, Hellebrekers LJ. Dexmedetomidine
691 continuous rate infusion during isoflurane anaesthesia in canine surgical patients.
692 *Vet Anaesth Analg*. 2008;**35**: 1-12.
693   46.   Ebner LS, Lerche P, Bednarski RM, Hubbell JA. Effect of dexmedetomidine,
694 morphine-lidocaine-ketamine,   and   dexmedetomidine-morphine-lidocaine-
695 ketamine constant rate infusions on the minimum alveolar concentration of
696 isoflurane and bispectral index in dogs. *American journal of veterinary research*.
697 2013;**74**: 963-970.
698   47.   Congdon JM, Marquez M, Niyom S, Boscan P. Cardiovascular, respiratory,
699 electrolyte and acid-base balance during continuous dexmedetomidine infusion in
700 anesthetized dogs. *Vet Anaesth Analg*. 2013;**40**: 464-471.
701   48.   Steagall PV, Teixeira Neto FJ, Minto BW, Campagnol D, Correa MA.
702 Evaluation of the isoflurane-sparing effects of lidocaine and fentanyl during surgery
703 in dogs. *Journal of the American Veterinary Medical Association*. 2006;**229**: 522-
704 527.
705   49.   Aguado D, Benito J, Gomez de Segura IA. Reduction of the minimum
706 alveolar concentration of isoflurane in dogs using a constant rate of infusion of
707 lidocaine-ketamine in combination with either morphine or fentanyl. *Vet J*.
708 2011;**189**: 63-66.
709   50.   Sano T, Nishimura R, Kanazawa H, Igarashi E, Nagata Y, Mochizuki M, et
710 al. Pharmacokinetics of fentanyl after single intravenous injection and constant rate
711 infusion in dogs. *Vet Anaesth Analg*. 2006;**33**: 266-273.
712   51.   Grimm KA, Tranquilli WJ, Gross DR, Sisson DD, Bulmer BJ, Benson GJ, et
713 al. Cardiopulmonary effects of fentanyl in conscious dogs and dogs sedated with
714 a continuous rate infusion of medetomidine. *American journal of veterinary*
715 *research*. 2005;**66**: 1222-1226.
716   52.   Keating SC, Kerr CL, Valverde A, Johnson RJ, McDonell WN.
717 Cardiopulmonary effects of intravenous fentanyl infusion in dogs during isoflurane
718 anesthesia and with concurrent acepromazine or dexmedetomidine administration
719 during anesthetic recovery. *American journal of veterinary research*. 2013;**74**: 672-
720 682.
721   53.   Seddighi R, Egger CM, Rohrbach BW, Cox SK, Doherty TJ. The effect of
722 midazolam on the end-tidal concentration of isoflurane necessary to prevent
723 movement in dogs. *Vet Anaesth Analg*. 2011;**38**: 195-202.
724   54.   Jones DJ, Stehling LC, Zauder HL. Cardiovascular responses to diazepam
725 and midazolam maleate in the dog. *Anesthesiology*. 1979;**51**: 430-434.
726   55.   Heniff MS, Moore GP, Trout A, Cordell WH, Nelson DR. Comparison of
727 routes of flumazenil administration to reverse midazolam-induced respiratory
728 depression in a canine model. *Acad Emerg Med*. 1997;**4**: 1115-1118.
729   56.   Bosiack AP, Mann FA, Dodam JR, Wagner-Mann CC, Branson KR.
730 Comparison of ultrasonic Doppler flow monitor, oscillometric, and direct arterial
731 blood pressure measurements in ill dogs. *J Vet Emerg Crit Care (San Antonio)*.
732 2010;**20**: 207-215.
733   57.   Hou DJ, Tso DK, Davison C, Inacio J, Louis LJ, Nicolaou S, et al. Clinical
734 utility of ultra high pitch dual source thoracic CT imaging of acute pulmonary

735 embolism in the emergency department: Are we one step closer towards a non-
736 gated triple rule out? *Eur J Radiol.* 2013;**82**: 1793-1798.
737 58.   Saremi F, Grizzard JD, Kim RJ. Optimizing cardiac MR imaging: practical
738 remedies for artifacts. *Radiographics : a review publication of the Radiological
739 Society of North America, Inc.* 2008;**28**: 1161-1187.
740 59.   Merin RG, Bernard JM, Doursout MF, Cohen M, Chelly JE. Comparison of
741 the effects of isoflurane and desflurane on cardiovascular dynamics and regional
742 blood flow in the chronically instrumented dog. *Anesthesiology.* 1991;**74**: 568-574.
743 60.   Francois CJ, Fieno DS, Shors SM, Finn JP. Left ventricular mass: manual
744 and automatic segmentation of true FISP and FLASH cine MR images in dogs and
745 pigs. *Radiology.* 2004;**230**: 389-395.
746 61.   Koren MJ, Devereux RB, Casale PN, Savage DD, Laragh JH. Relation of
747 left ventricular mass and geometry to morbidity and mortality in uncomplicated
748 essential hypertension. *Ann Intern Med.* 1991;**114**: 345-352.
749 62.   Shors SM, Fung CW, Francois CJ, Finn JP, Fieno DS. Accurate
750 quantification of right ventricular mass at MR imaging by using cine true fast
751 imaging with steady-state precession: study in dogs. *Radiology.* 2004;**230**: 383-
752 388.
753 63.   Levy D, Garrison RJ, Savage DD, Kannel WB, Castelli WP. Prognostic
754 implications of echocardiographically determined left ventricular mass in the
755 Framingham Heart Study. *The New England journal of medicine.* 1990;**322**: 1561-
756 1566.
757 64.   Devereux RB. Detection of left ventricular hypertrophy by M-mode
758 echocardiography. Anatomic validation, standardization, and comparison to other
759 methods. *Hypertension.* 1987;**9**: II19-26.
760 65.   Devereux RB, Reichek N. Echocardiographic determination of left
761 ventricular mass in man. Anatomic validation of the method. *Circulation.* 1977;**55**:
762 613-618.
763 66.   Juergens KU, Seifarth H, Range F, Wienbeck S, Wenker M, Heindel W, et
764 al. Automated threshold-based 3D segmentation versus short-axis planimetry for
765 assessment of global left ventricular function with dual-source MDCT. *AJR
766 American journal of roentgenology.* 2008;**190**: 308-314.
767 67.   Fratz S, Schuhbaeck A, Buchner C, Busch R, Meierhofer C, Martinoff S, et
768 al. Comparison of accuracy of axial slices versus short-axis slices for measuring
769 ventricular volumes by cardiac magnetic resonance in patients with corrected
770 tetralogy of fallot. *Am J Cardiol.* 2009;**103**: 1764-1769.
771 68.   Folland ED, Parisi AF, Moynihan PF, Jones DR, Feldman CL, Tow DE.
772 Assessment of left ventricular ejection fraction and volumes by real-time, two-
773 dimensional echocardiography. A comparison of cineangiographic and
774 radionuclide techniques. *Circulation.* 1979;**60**: 760-766.
775 69.   Sanz J, Conroy J, Narula J. Imaging of the right ventricle. *Cardiol Clin.*
776 2012;**30**: 189-203.
777 70.   Sousa MG, Carareto R, De-Nardi AB, Brito FL, Nunes N, Camacho AA.
778 Effects of isoflurane on echocardiographic parameters in healthy dogs. *Vet
779 Anaesth Analg.* 2008;**35**: 185-190.

780   71.   Hettrick DA, Pagel PS, Warltier DC. Isoflurane and halothane produce
781   similar alterations in aortic distensibility and characteristic aortic impedance.
782   *Anesth Analg.* 1996;**83**: 1166-1172.
783
784

785

786

787

788

789

790

791

792

793

794

795

796 Tables

797 Table 1: Summary of the Vital Variables Recorded during MDCTA and MRI Exams using Protocol A (Midazolam/Fentanyl)

798 and Protocol B (Dexmedetomedine) in ten dogs. *

	Protocol A	Protocol B
	Median	Median
	(min-max)	(min-max)
CT		
heart rate (bpm)	81.6	73.3
	(68.6-96)	(62.7-102.6)
mean blood pressure (mmHg)	65.0	65.3
	(48.8-74.0)	(57-102.8)*
systolic arterial pressure (mmHg)	92.5	92.7
	(74.3-100.4)	(81.0-129.8)
diastolic arterial pressure (mmHg)	37.6	44.2
	(28.2-47.2)	(31.8-75.8)*

CO2 (%)	39.7	35.5
	(34.7-46.7)	(34.7-45.0)
MRI		
heart rate (bpm)	76.8	71
	(66-98.6)	(64.4-118.8)
mean blood pressure (mmHg)	60.5	75.3
	(48.4-68.9)	(66.1-94.0)
systolic arterial pressure (mmHg)	89.1	101.9
	(75.3-95.6)	(91.7-117.6)
diastolic arterial pressure (mmHg)	36.2	51.9
	(29.2-43.4)	(30.9-72.5)
CO2 (%)	37.5	34.1
	(34.3-45.8).	(30.6-37.0)

799

800   *When comparing Protocol A and B there was significant difference for the mean (P = 0.012), diastolic arterial (P = 0.033)

801   and marginal difference for the systolic arterial blood pressure (P = 0.052). For the remaining variables no difference was

802   found (heart rate, CO_2; P = 1).

803

804

805 Table 2: Volumetric Measurements Generated from the Echocardiograms Obtained in the Ten Dogs Awake as well as the

806 cardiac 64-MDCTA and 3T MRI Exams Using Anesthetic Protocol A and Protocol B.

807

Modality	Echocardiography	MDCTA		MRI	
Anesthetic protocol	Awake	Protocol A	Protocol B	Protocol A	Protocol B
		Median	Median	Median	Median
		(min-max)	(min-max)	(min-max)	(min-max)
LVEDV (ml)	42.5	34.7	37.8	38.1	36.2
	(29.0-56.0)*	(26.9-41.1)	(26.6-43.2)[†]	(30.0-45.2)	(26.7-45.1)
LVESV (ml)	15.5	16.9	17.0	17.8	18.75
	(8.0-21.0)*	(8.8-25.2)	(14.8-26.8)	(13.0-25.8)	(12.9-25.8)
LSV (ml)	25.5	17.2	18.2	19.5	17.6
	(19.0-39.0)*	(15.2-25.1)	(11.7-22.5)	(15.4-22.1)	(9.9-26.0)
LVEF (%)	62.0	52.5	47.3	52.8	43.9
	(51.0-79.0)*	(37.7-71.1)	(36.2-60.3)	(42.9-59.7)	(33.8-64.5)

LVmassD (mg)	60.2	39.4	38.6	39.4	39.4
	(30.7-68.4)	(27.7-46.4)	(28.2-44.1)	(27.5-45.7)	(26.7-48.7)
LVmass (mg)	NA	39.1	37.0	39.1	40.1
		(26.9-47.2)	(28.5-44.8)	(28.7-47.3)	(27.8-43.3)
RVEDV (ml)	NA	36.8	35.6	42.7	40.2
		(29.2-41.1)	(27.2-44.4)	(32.2-50.9)	(30.1-50.5)
RVESV (ml)	NA	22.4	21.9	22.5	25.4
		(14.6-28.7)	(14.9-32.5)	(15.5-29.1)	(15.1-30.6)
RVSV (ml)	NA	14.5	12.2	18.5	16.2
		(8.2-20.3)	(7.3-21.3)	(14.6-25.3)	(8.1-22.7)
RVEF (%)	NA	40.0	37.4	45.2	43.3
		(22.3-55.1)	(23.6-48.2)	(38.6-58.2)	(23.6-50.0)

808

809   *Simpson's Method, [†]P-value for comparison of echocardiography and MDCT for LVEDV

810   = 0.01, all other P-values are greater than 0.05 or N/A.

811

812   LVEDV = left ventricular end diastolic volume; LVESV = left ventricular end systolic

813   volume; LSV = left ventricular stroke volume; LVEF = left ventricular ejection fraction;

814   LVmassD = diastolic left ventricular myocardial mass; LVmassS = systolic left ventricular

815   myocardial mass; RVEDV = right ventricular end diastolic volume; RVESV = right

816   ventricular end systolic volume; RVSV = right ventricular stroke volume; RVEF = right

817   ventricular ejection fraction

818

819

820

821

822

823

824

825

826

827

828

829

830

831

832 Table 3: Planar Measurements Generated from the Echocardiographic Exam Obtained

833 in the Ten Dogs Awake as well as Cardiac 64-MDCTA and 3T MRI Exams Using Protocol

834 A and B.*

835

836

837

838

839

840

841

842

843

844

845

846

847

848

849

Modality	Echo	CTA		MRI	
Anesthetic protocol	Awake	Protocol A	Protocol B	Protocol A	Protocol B
	Median	Median	Median	Median	Median
	(min-max)	(min-max)	(min-max)	(min-max)	(min-max)
IVSd (cm)	0.76	0.73	0.74	0.79	0.77
	(0.66-0.88)	(0.52-0.79)	(0.49-0.82)	(0.66-1.02)	(0.59-0.98)
IVSs (cm)	1.06	0.8	0.85	0.94	0.77
	(0.95-1.2)	(0.58-0.95)	(0.61-0.96)	(0.66-1.47)	(0.54-1.04)
LVIDd (cm)	3.25	2.97	2.98	3.19	3.41
	(2.79-3.63)	(2.69-3.31)	(2.78-3.35)	(2.97-3.45)	(2.84-3.63)
LIVDs (cm)	2.15	2.56	2.64	2.6	2.67
	(1.67-2.45)	(2.23-2.76)	(2.35-3.03)	(2.04-2.96)	(2.23-3.07)
LVPWd (cm)	0.68	0.75	0.75	0.76	0.73
	(0.53-0.79)	(0.6-1.0)	(0.66-0.84)	(0.52-0.94)	(0.7-0.94)
LVPWs (cm)	1.03	1.0	0.9	1.04	0.92
	(0.85-1.17)	(0.72-1.23)	(0.72-1.0)	(0.46-1.25)	(0.65-1.22)

FS (%)	33.5	13.11	12.08	21.5	16.81
	(26.0-41.0)	(6.88-25.22)	(3.53-20.22)	(12.11-32.44)	(11.85-29.53)
LA diam 3ch (cm)	2.21	2.93	2.99	2.8	2.72
	(1.92-2.49)	(2.62-3.24)	(2.63-3.34)	(2.10-2.92)	(2.41-2.99)
Mitral annulus 3ch (mm)	NA	2.01	1.93	2.02	1.94
		(1.82-2.08)	(1.5-2.2)	(1.71-2.34)	(1.83-2.20)
Ao annulus 3ch (%)	1.71	1.3	1.3	1.17	1.18
	(1.55-1.97)*	(0.99-1.37)	(1.09-1.38)	(0.94-1.47)	(1.04-1.34)
LA/Ao ratio	1.27	2.34	2.34	2.41	2.35
	(1.18-1.49)	(1.97-3.05)	(1.97-3.05)	(1.93-3.04)	(1.8-2.64)
Mitral annulus diam 4ch (cm)	NA	2.4	2.4	2.13	2.04
		(2.12-2.58)	(2.19-2.69)	(1.69-2.23)	(1.8-2.34)
prox Ao (cm)	NA	1.27	1.28	1.28	1.32
		(1.14-1.52)	(1.08-1.51)	(1.07-1.6)	(1.18-1.56)
MPA (cm)	1.6	1.39	1.33	1.23	1.3
	(1.5-1.8) [†]	(1.21-1.56)	(0.92-1.56)	(1.11-1.24)	(1.12-1.56)

Ao/PA ratio	0.99	0.96	0.96	1.03	1.09
	(0.86-1.31)	(0.82-1.04)	(0.8-1.48)	(0.96-1.22)	(0.98-1.19)

850

851   IVSd = diastolic interventricular septal thickness; IVSs = systolic interventricular

852   septal thickness; LVIDd = diastolic left ventricular internal diameter, measured

853   just proximal to the papillary muscles; LVIDs = systolic left ventricular internal

854   diameter, measured just proximal to the papillary muscles; LVPWd = diastolic left

855   ventricular posterior wall thickness; LVPWs = systolic left ventricular posterior

856   wall thickness; FS% = percent fractional shortening; LA diam 3ch = left atrial

857   diameter measured on three chamber view; Mitral annulus 3ch = mitral annulus

858   measured on approximated three-chamber view; Ao annulus 3ch = aortic

859   annulus measured on three-chamber view; LA/Ao ratio = Left atrium to aorta

860   ratio; Mitral annulus 4ch = mitral annulus measured on four-chamber view; prox

861   Ao = Proximal aorta measured on transverse plane; MPA = main pulmonary

862   artery transverse plane; Ao/PA ratio = Aorta to pulmonary artery ratio. *Aortic

863   annulus measured in right parasternal view for the left ventricular outflow tract on

864   echocardiography; [†] MPA measured in right parasternal short axis view on

865   echocardiography

866   [‡]No statistically significant differences were found between the anesthetic

867   protocols within the cross-sectional modalities using the paired Wilcoxon rank

868   sum test ($P = 0.292$ for LVIDs using MRI; $P = 1$ for all other variables). The

869   cross-sectionally acquired measurements did not allow for prediction of the

870   values generated using echocardiography in the awake dogs ($P = 1$ for all

871   variables).

872

873

874

875

876

877

878

879

880

881 Table 4: Results of the Bland-Altman Analysis Characterizing the Differences for
882 the Volumetric Measurements Between the 64-MDCTA and 3T MRI Exams (MRI
883 minus CT) When Combining the Results of the two Anesthetic Protocols per
884 Modality and Individual.

885

Volumetric cardiac variable	LLOA	Bias	ULOA
LVEDV (ml)	-5.43	1.42	8.27
LVESV (ml)	-4.28	1.37	7.02
LSV (ml)	-6.84	0.05	6.94
LVEF (%)	-17.45	-2.11	13.24
LVmassD (mg)	-6.51	2.05	10.62
LVmassS (mg)	-5.33	1.62	8.58
RVEDV (ml)	-6.87	5.08	17.04
RVESV (ml)	-7.88	0.89	9.66
RVSV (ml)	-3.63	4.19	12.02
RVEF (%)	-9.54	5.51	20.57

886 LLOA = 95% lower level of agreement; ULOA = 95% upper level of agreement;

887 LVEDV = left ventricular end diastolic volume; LVESV = left ventricular end systolic

888 volume; LSV = left ventricular stroke volume; LVEF = left ventricular ejection

889 fraction; LVmassD = diastolic left ventricular myocardial mass; LVmassS = systolic

890 left ventricular myocardial mass; RVEDV = right ventricular end diastolic volume;

891   RVESV = right ventricular end systolic volume; RVSV = right ventricular stroke

892   volume; RVEF = right ventricular ejection fraction.

893

894

895

896

897

898

899

900

901

902

903

904

905

906

907

908

909

910

911

912

913

914 Table 5: Bias and 95% Upper (ULOA) and Lower Level of Agreement (ULOA)

915 Generated by the Comparison of the Planar Variables Acquired using 64-MDCTA

916 and 3T MRI (MRI minus CT) using the Bland-Altman Analysis are Reported.

917

Planar variable	LLOA	Bias	ULOA
IVSd (cm)	- 0.19	0.08	0.35
IVSs (cm)	- 0.29	0.09	0.46
LVIDd (cm)	- 0.15	0.21	0.56
LIVDs (cm)	- 0.49	- 0.01	0.47
LVPWd (cm)	- 0.21	- 0.01	0.18
LVPWs (cm)	- 0.42	0.0	0.42
FS (%)	- 9.29	5.94	21.18
LA diam (cm)	- 0.37	- 0.3	0.18
Mitral annulus 3ch (cm)	- 0.31	0.04	0.38
Ao annulus 3ch (cm)	- 0.37	- 0.1	0.18
LA/Ao ratio	- 0.88	- 0.01	0.86
Mitral annulus 4ch (cm)	- 0.8	- 0.35	0.09
prox Ao (cm)	- 0.16	0.02	0.21
MPA (cm)	- 0.45	- 0.09	0.27
Ao/PA ratio (cm)	- 0.19	0.08	0.65
Mitral annulus: 3ch vs 4ch (cm)	- 0.29	0.27	0.83

918

919   Overall good agreement was found between the modalities when combining the

920   anesthetic protocols per modality and individual.

921

922   LLOA = lower level of agreement; ULOA = upper level of agreement; IVSd =

923   diastolic interventricular septal thickness; IVSs = systolic interventricular septal

924   thickness; LVIDd = diastolic left ventricular internal diameter, measured just

925   proximal to the papillary muscles; LVIDs = systolic left ventricular internal

926   diameter, measured just proximal to the papillary muscles; LVPWd = diastolic left

927   ventricular posterior wall thickness; LVPWs = systolic left ventricular posterior

928   wall thickness; FS% = percent fractional shortening; LA diam 3ch = left atrial

929   diameter measured on three chamber view; Mitral annulus 3ch = mitral annulus

930   measured on approximated three-chamber view; Ao annulus 3ch = aortic

931   annulus measured on three-chamber view; LA/Ao ratio = Left atrium to aorta

932   ratio; Mitral annulus 4ch = mitral annulus measured on four-chamber view; prox

933   Ao = Proximal aorta measured on transverse plane; MPA = main pulmonary

934   artery transverse plane; Ao/PA ratio = Aorta to pulmonary artery ratio

935

936

937

938

939

940

941

942 Figures

943
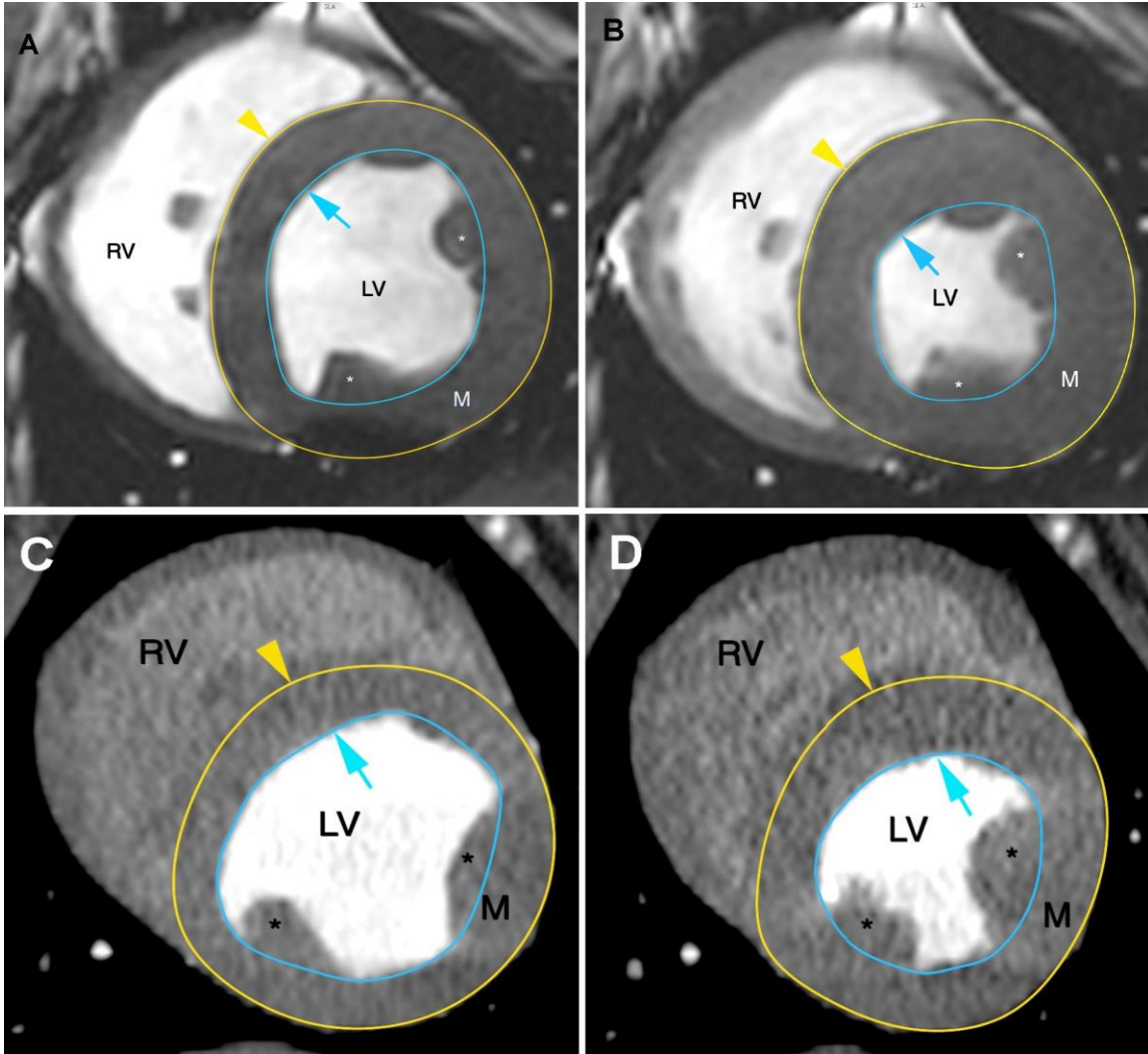
Figure1: Using the short axis plane the epicardial (yellow line, arrow head) and endocardial (turquoise line, arrow) surface of the left ventricle (LV) were outlined on all images including the left ventricle to calculate the volumetric variables; each at the end diastolic (A, C) and end systolic (B, D) phase for MDCTA and MRI respectively; exemplary views are given at the level of the papillary muscles. Papillary muscles (*) were included in the left ventricular volume. RV = right ventricle.

951
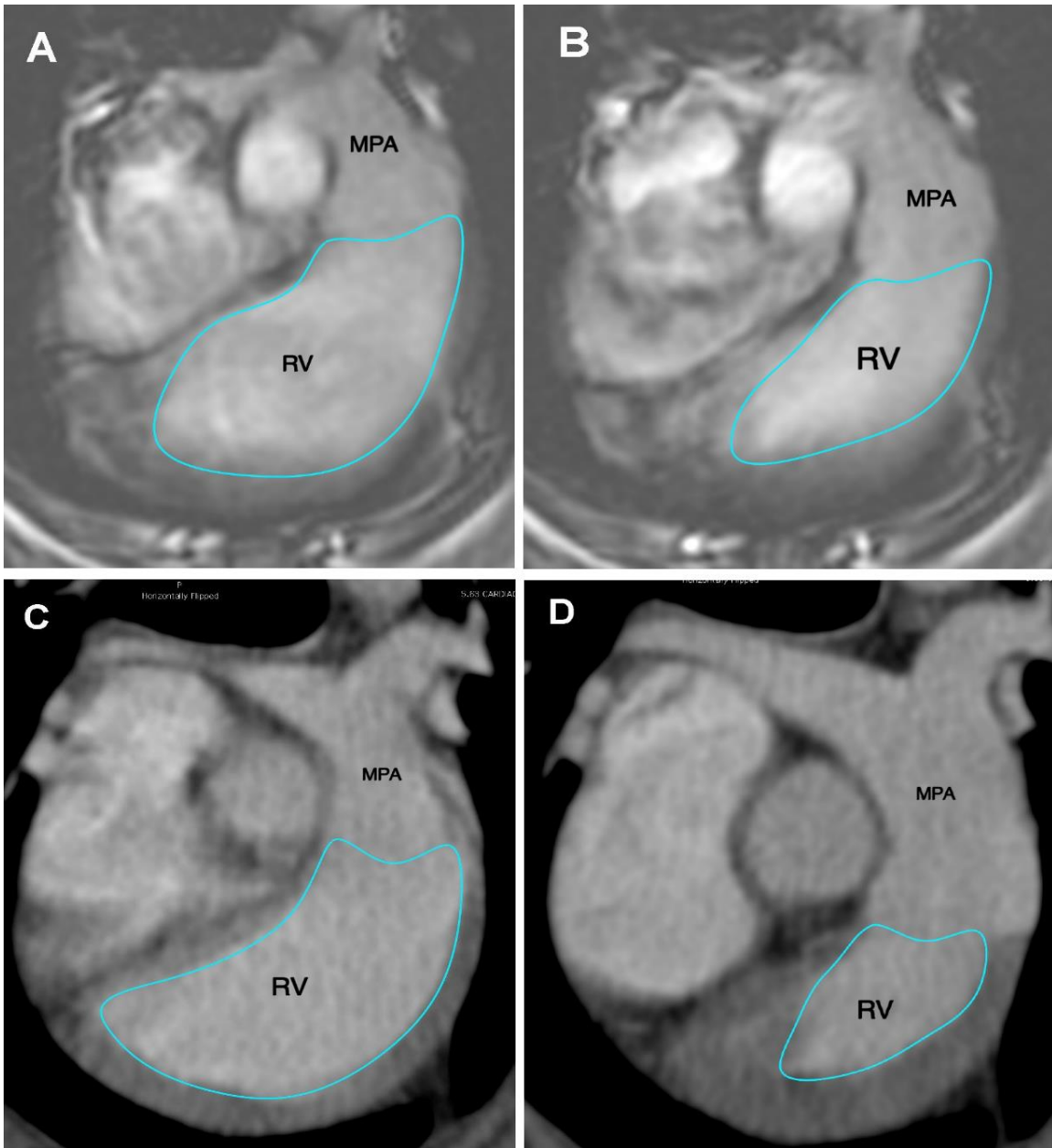
Figure 2: Using transverse plane images the endocardial surface (turquoise line) of the right ventricle (RV) was outlined on all images including the right ventricle, where the tricuspid and pulmonic annulus marked the borders of the ventricular volume included. This was performed at the end diastolic (A, C) and end systolic (B, D) phase for MDCTA and MRI respectively; exemplary views are given at the level of the right ventricular outflow tract. MPA = main pulmonary artery.
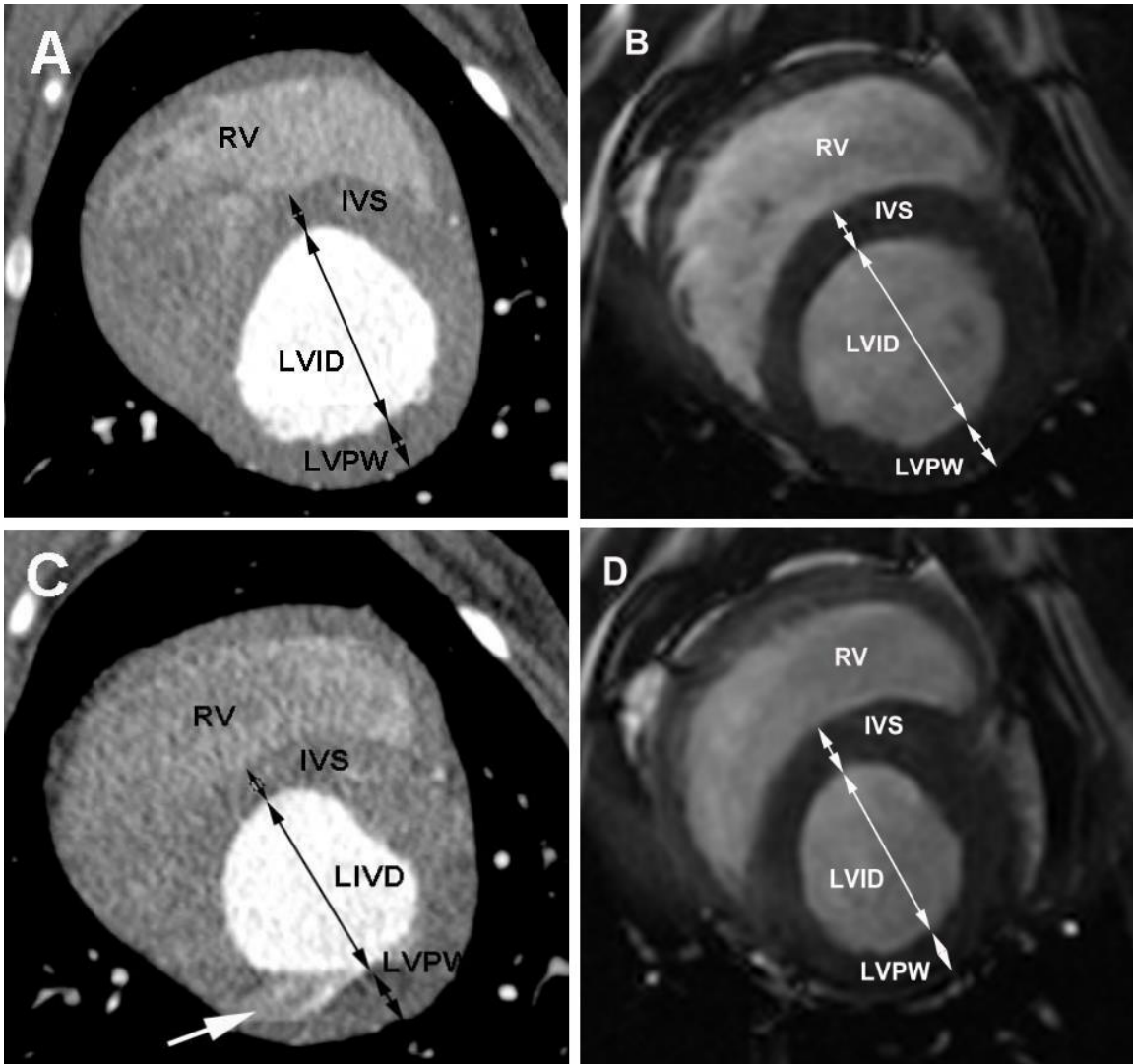
959

960 Figure 3: Short axis view of the left ventricle end diastolic (A, C) and end systolic

961 (B, D) using MDCTA and MRI respectively, showing the measurement of IVS

962 (interventricular septum) and LVPW (left ventricular posterior wall) thickness and

963 LVID (left ventricular internal diameter) using double-headed arrows. Single-

964 headed arrow showing mild motion artifact in end systole, this did not interfere with

965 placement of measurements. RV = Right ventricle.
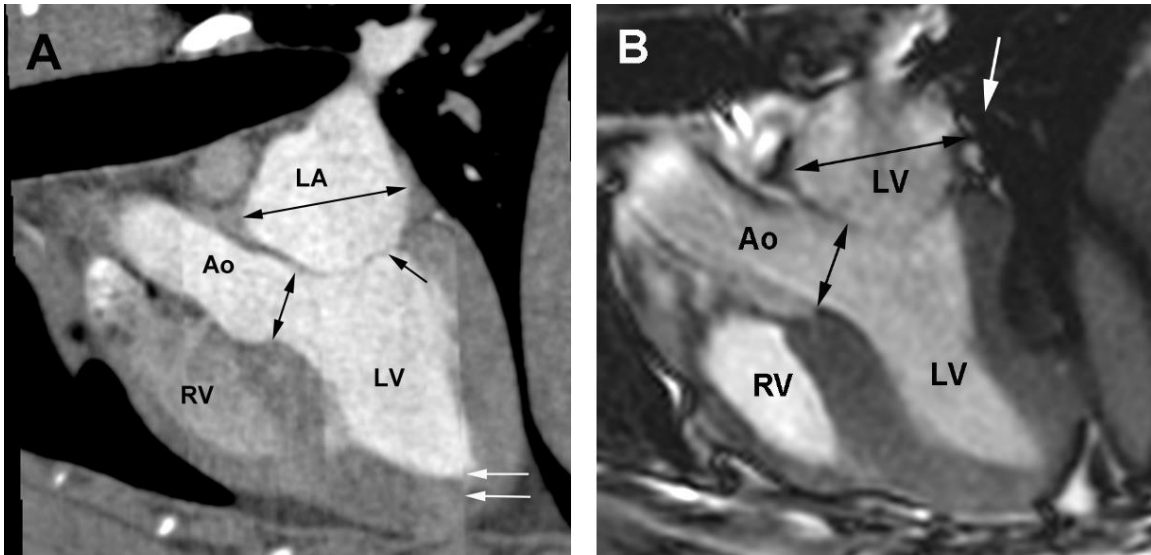
966

967 Figure 4: End systolic three-chamber view generated using MDCTA (A) and MRI

968 (B) respectively for measurement of the left atrial (light blue line) and aortic annulus

969 (dark blue line) diameter. Mitral valves (green arrows) are closed, aortic valves are

970 open. There is mild flow artefact on the MRI image over the caudal aspect of the

971 left atrium (yellow arrow) arising from inflow from the pulmonary veins and mild

972 motion artefact over the caudal aspect of the left ventricle (yellow arrows) over the

973 left ventricle on the MDCTA image. LA = left atrium; LV = left ventricle; RV = right

974 ventricle; Ao = aorta.

975
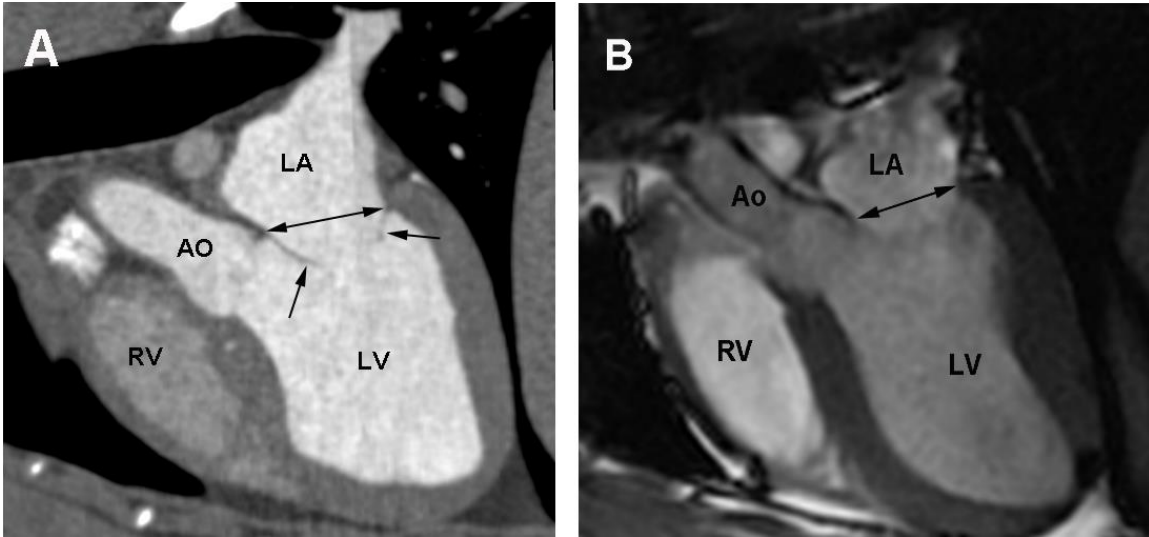
976

977 Figure 5: End diastolic three-chamber view generated using MDCTA (A) and MRI

978 (B) respectively for measurement of the mitral annulus diameter measurement

979 (light blue and yellow respectively). Mitral valves are open (green arrow). LA = left

980 atrium; LV = left ventricle; RV = right ventricle; Ao = aorta.

981

982
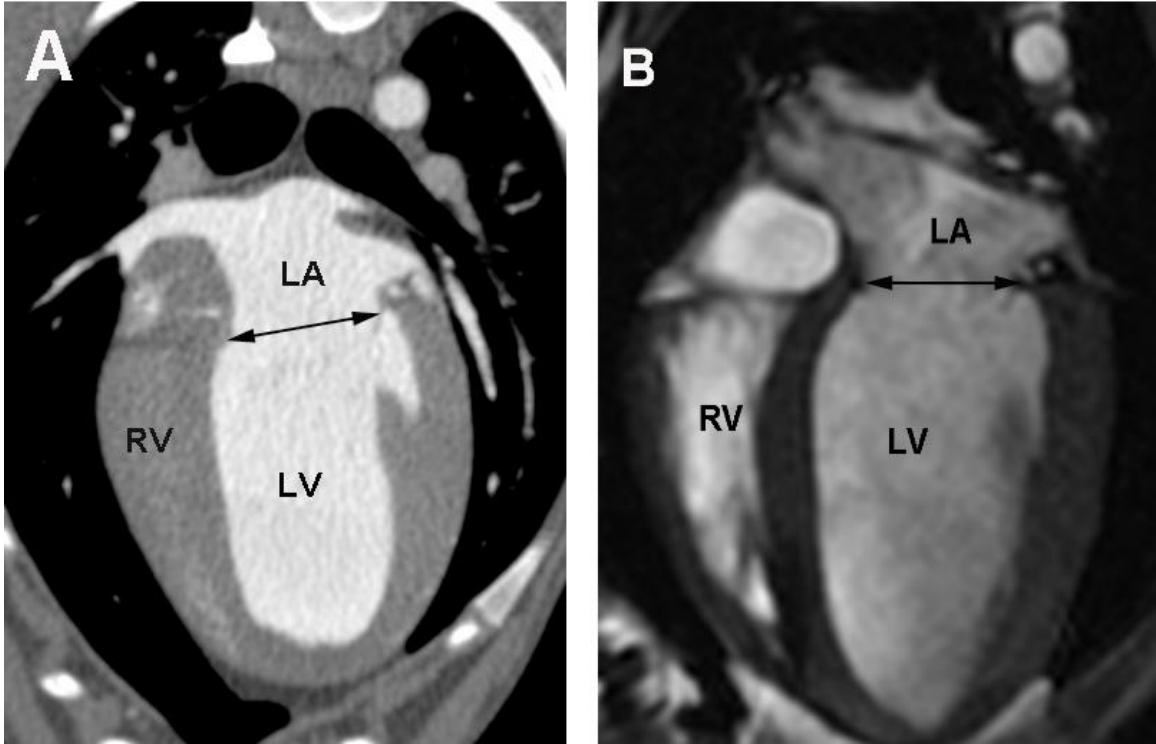
Figure 6: Approximate four-chamber view using MDCTA (A) and MRI (B) for repeat

measurement of the mitral annulus diameter (light blue line) at end diastole. LA =

left atrium; LV = left ventricle; RV = right ventricle.

986
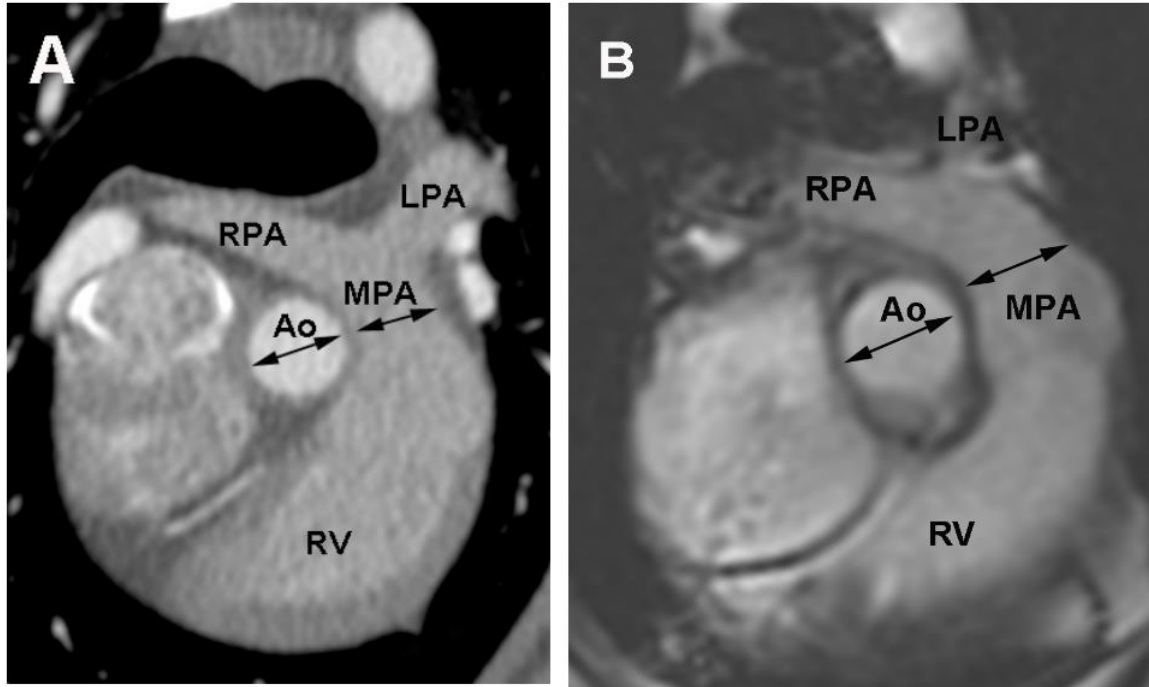
987

988 Figure 7: Transverse plane view using MDCTA (A) and MRI (B) respectively for

989 measurement of the diameter of the proximal aorta (Ao, blue line) and the main

990 pulmonary artery (MPA, yellow line). RPA = right pulmonary artery; LPA = left

991 pulmonary artery; RV = right ventricle.

LVEDV

LVESV

LVmassD

LVmassS

LVSV

LVEF

992
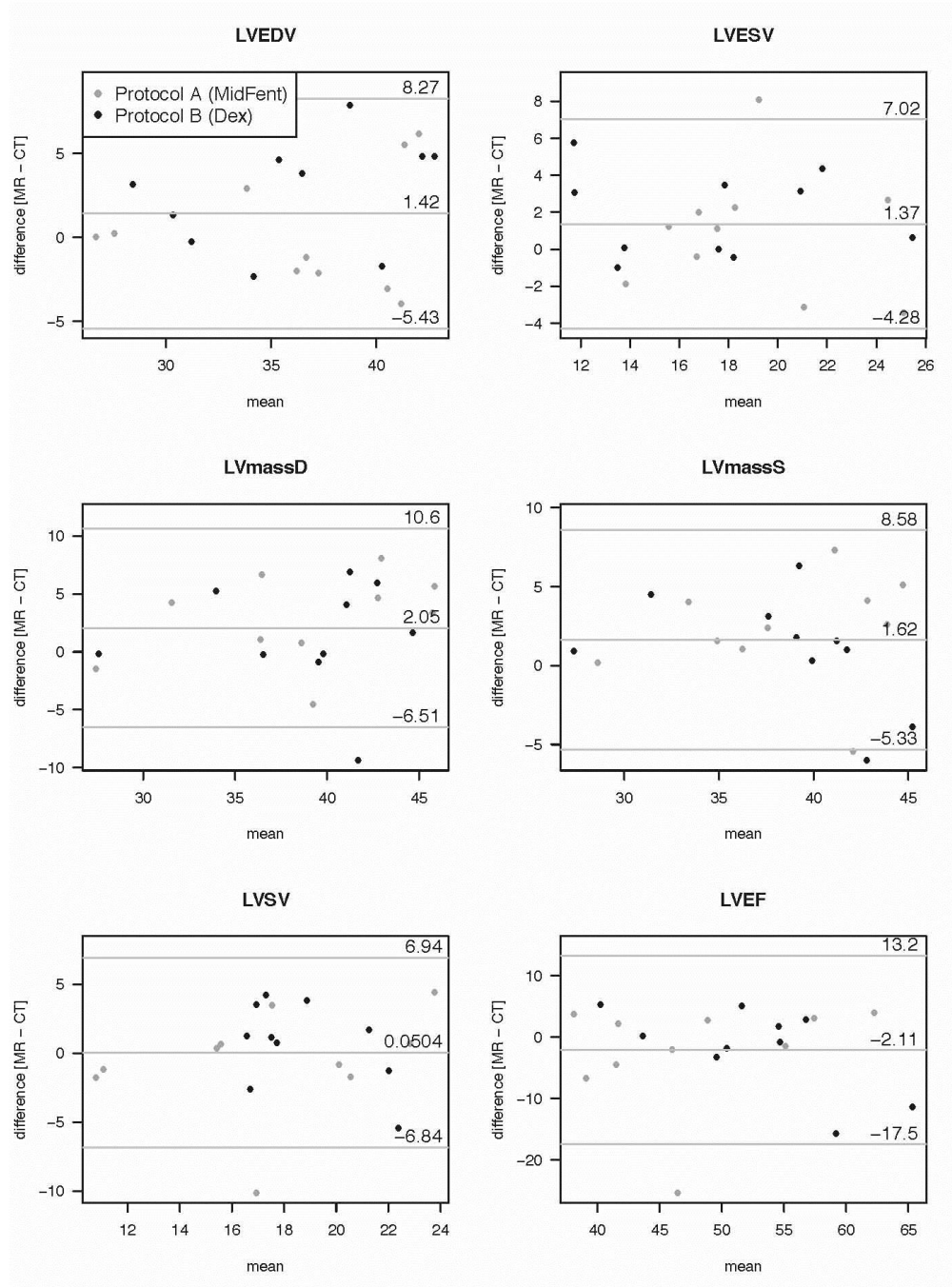
Figure 8: Graphical display of the Bland-Altman analysis comparing the left ventricular volumetric measurements generated using 64-MDCTA (CT) versus 3T-MRI (MR) while combining the measures for the two different anesthetic episodes per modality. The bias is given by the central horizontal line, the 95% lower and

997 upper level of agreement are indicated by the above and below horizontal lines.

998 LVEDV: Left Ventricular End Diastolic Volume (ml); Left Ventricular End Systolic

999 Volume (ml); LVmassD: Left Ventricular Myocardial Mass at Diastole (mg);

1000 LVmassS: Left Ventricular Myocardial Mass at Systole (mg); LVSV: Left

1001 Ventricular Stroke Volume (ml); LVEF: Left Ventricular Ejection Fraction (ml). Dex

1002 = Anesthetic Protocol B; MidFent = Anesthetic Protocol A.
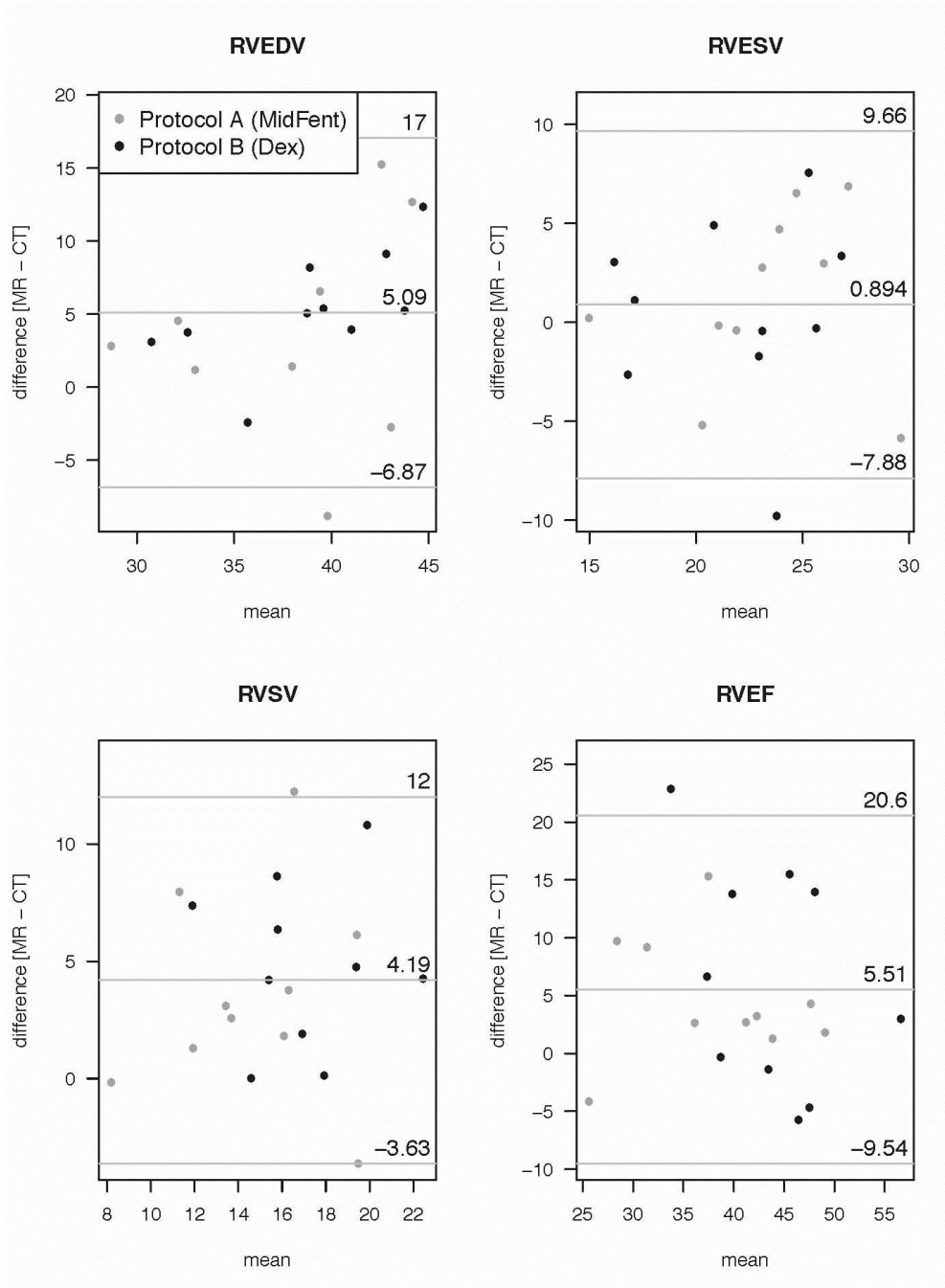
1003

Figure 9: Graphical display of the Bland-Altman analysis comparing the right ventricular volumetric measurements generated using MDCTA versus MRI while combining the measures for the two different anesthetic episodes per modality. The bias is given by the center horizontal line, the 95% lower and upper level of agreement are indicated by the above and below horizontal lines. RVEDV: Right

1009   Ventricular End Diastolic Volume (ml); RVESV: Right Ventricular End Systolic

1010   Volume (ml); RVSV: Right Ventricular Stroke Volume (ml); RVEF: Right Ventricular

1011   Ejection Fraction (ml). Dex=Anesthetic Protocol B; MidFent=Anesthetic Protocol

1012   A.

1013
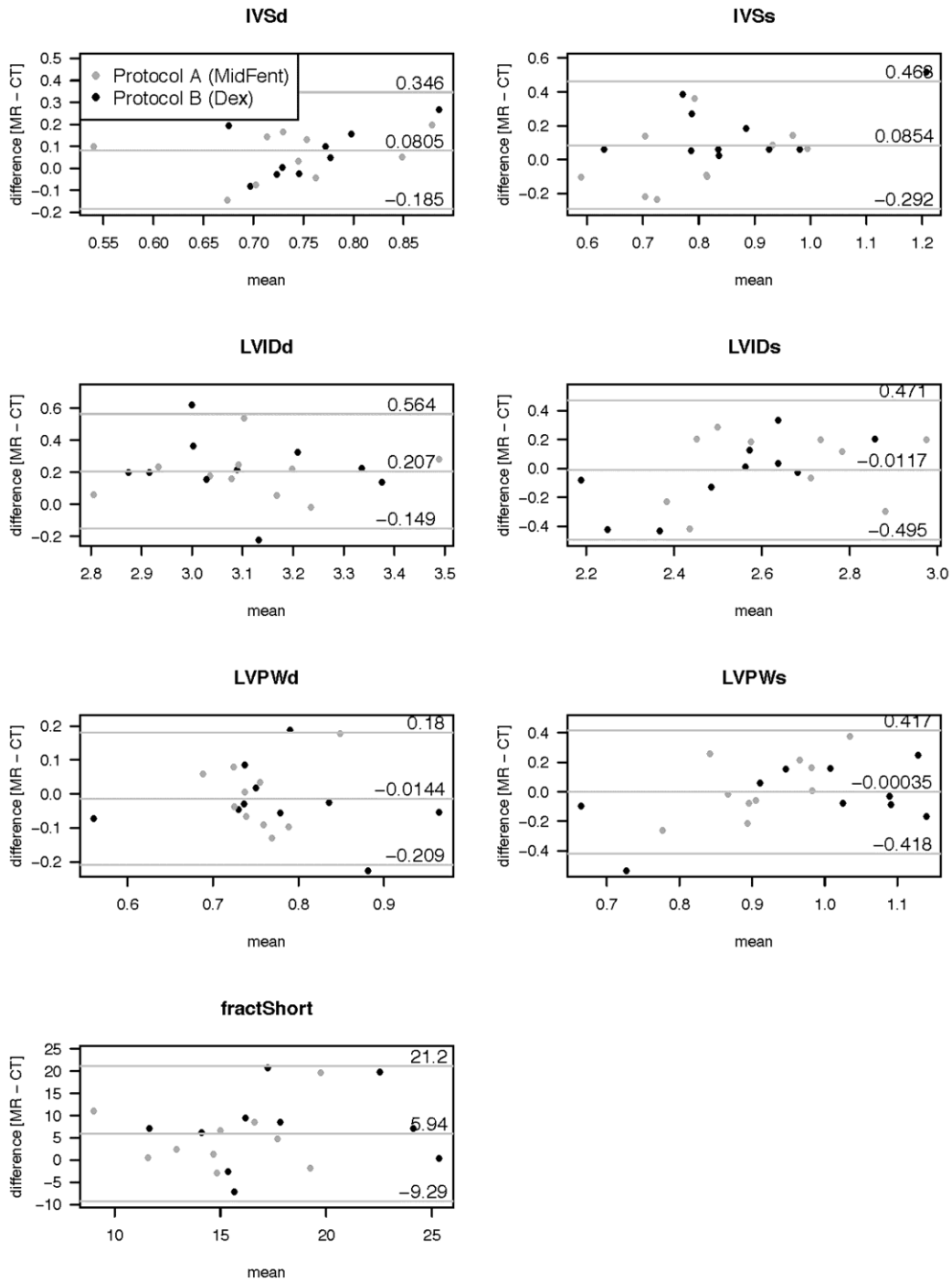
1014

1015 Figure 10: Graphical display of the Bland-Altman analysis comparing the planar

1016 left ventricular measurement generated using MDCTA (CT) versus MRI (MR) when

1017 combining the measures for the two different anesthetic episodes per modality.

1018   The bias is shown by the central horizontal line, the 95% lower and upper levels of

1019   agreement are depicted as the horizontal lines above and below.

1020   IVSd: interventricular septum thickness at diastole (cm); IVSs: interventricular

1021   septum thickness at systole (cm); LVIDd: left ventricular internal diameter at

1022   diastole (cm); left ventricular internal diameter at systole (cm); LVPWd: left

1023   ventricular diameter at diastole (cm); LVPWs: left ventricular diameter at systole

1024   (cm); fractShort: fractional shortening (%)

1025
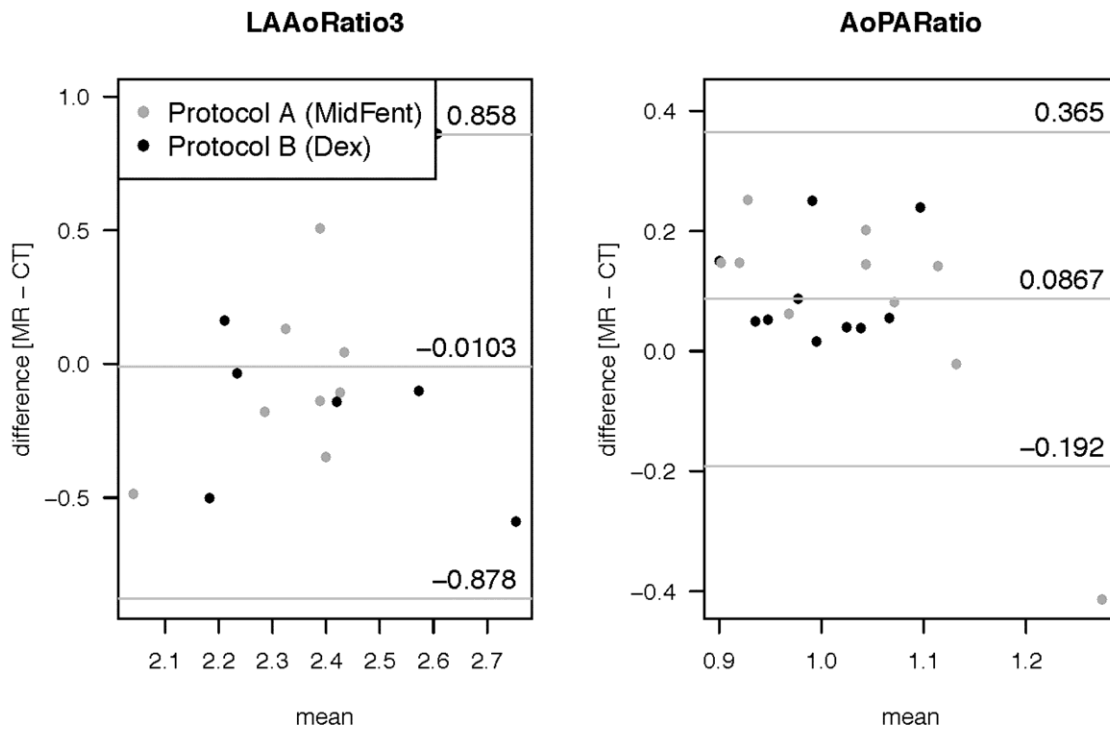
Figure 11: Graphical display of the Bland-Altman analysis comparing the LA/Ao-Ratio (left atrium (generated from three chamber view) to aorta ratio) and Ao/PA-Ratio (aorta to pulmonary artery ratio) generated from the planar measurements using MDCTA (CT) versus MRI (MR) when combining the measurements for the two different anesthetic episodes per modality. The bias is shown by the central horizontal line, the 95% lower and upper levels of agreement are depicted as the horizontal lines above and below.
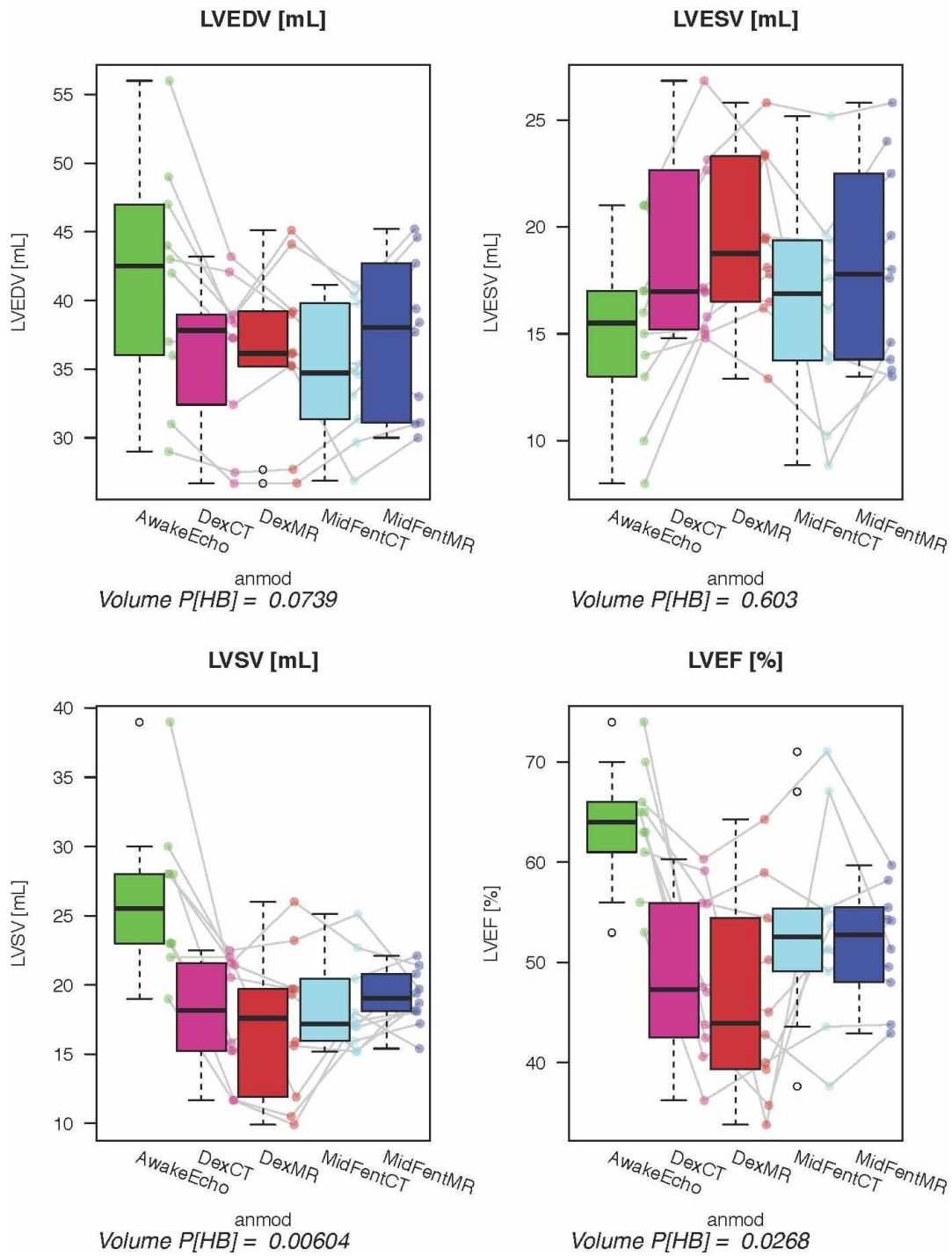
Figure 12: Graphical Display using Box-Pots to Compare the Volumetric Measurements acquired using the Anesthetic Protocol and Cross-sectional Modality Combinations to the Echocardiographic Results Gathered from the

1039 Awake Animals. Adjusted P-Values for all five exams (awake echocardiogram,

1040 anesthesia and MDCT, MRI using Protocol A, B) are given below the plots. Only

1041 LVEDV using MDCTA and anesthetic protocol B (P = 0.01) was able to allow for

1042 measurements generated using awake echocardiogram. LVEDV (ml): Left

1043 Ventricular End Diastolic Volume; LVESV (ml): Left Ventricular End Systolic

1044 Volume; LVSV (ml): Left Ventricular Stroke Volume; LVEF (%): Left Ventricular

1045 Ejection Fraction

1046 AwakeEcho = Echocardiogram performed on the awake dogs; DexCT = MDCTA

1047 using Anesthetic Protocol B; DexMR = MRI using Anesthetic Protocol B;

1048 MidFentCT = MDCTA using Anesthetic Protocol A; MidFentMR = MRI using

1049 Anesthetic Protocol A. Line segments join observations obtained from the same

1050 dog as imaging and anesthesia protocols vary.

1051

IVSd [cm]

2D P[HB] = 0.447 anmod

IVSs [cm]

2D P[HB] = 0.000639 anmod

LVIDd [cm]

2D P[HB] = 0.03 anmod

LVIDs [cm]

2D P[HB] = 0.00244 anmod

LVPWd [cm]

2D P[HB] = 0.755 anmod

LVPWs [cm]

2D P[HB] = 0.755 anmod

fractShort [%]

2D P[HB] = 0.000499 anmod
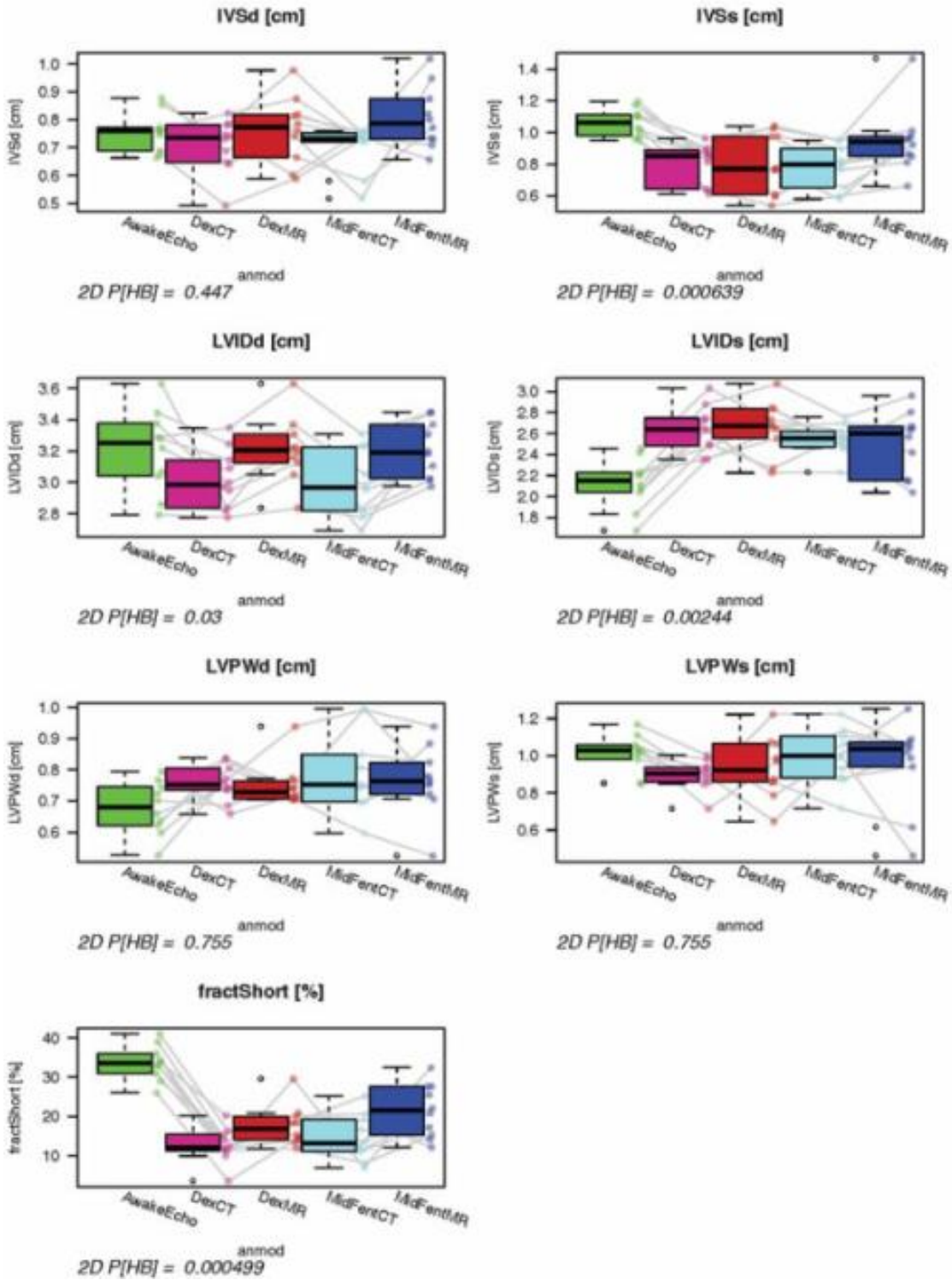
1052

1053   Figure 13: Graphical display using box-plots to compare left ventricular planar

1054   measurements generated using the four anesthetic protocol and modality

1055 combinations to the echocardiographic results gathered from the awake animals.

1056 No significant differences were found for any of the variables comparing the

1057 anesthesia protocols within each modality using paired Wilcoxon testing. Adjusted

1058 P-values comparing all five exams (awake echocardiogram, anesthesia and

1059 MDCT, MRI using Protocol A, B) are given below the plots. Prediction of

1060 echocardiographic measurements using the cross-sectional modalities was not

1061 possible (P =1).

1062 IVSd (cm): interventricular septal thickness at diastole; IVSs (cm): interventricular

1063 septal thickness at systole; LVIDd (cm): left ventricular internal diameter at

1064 diastole. Using protocol A and 64-MDCTA this was the only variable allowing for

1065 predictions of the echocardiographic measurement in the awake dog; LIVDs (cm):

1066 left ventricular internal diameter at systole; LVPWd (cm): left ventricular posterior

1067 wall at diastole; LVPWs (cm): left ventricular posterior wall at systole; FractShort

1068 (%): fractional shortening.

1069 AwakeEcho = echocardiogram performed on the awake dogs; DexCT = MDCTA

1070 using anesthetic protocol B; DexMR = MRI using anesthetic protocol B; MidFentCT

1071 = MDCTA using anesthetic protocol A; MidFentMR = MRI using anesthetic protocol

1072 A. Line segments join observations obtained from the same dog as imaging and

1073 anesthesia protocols vary.

1074

AoDiam3 [cm]

LADiam3 [cm]

2D P[HB] = 0.00436

2D P[HB] = 0.00344

PADiam [cm]

LAAoRatio3

2D P[HB] = 0.000863

2D P[HB] = 0.0421

AoPARatio

2D P[HB] = 0.0476
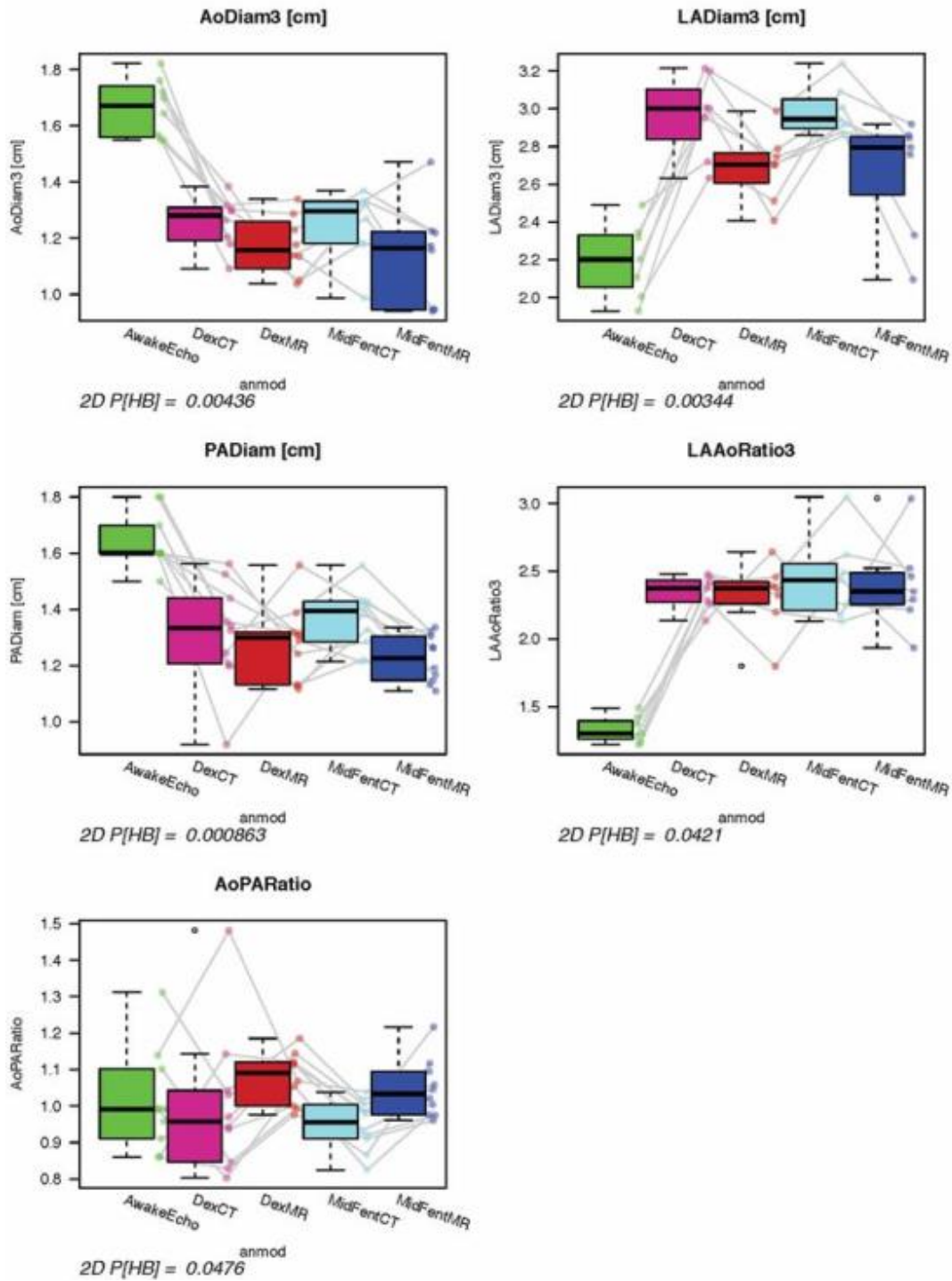
1075

1076 Figure 14: Graphical display using Box-Pots showing comparison of selected

1077 planar measurements generated using the four anesthetic protocol and modality

1078 combinations to the echocardiographic results gathered from the awake animals.

1079　There were no significant differences were found for any of the variables

1080　comparing the anesthesia protocols within each modality using paired Wilcoxon

1081　testing.　Adjusted P-values comparing all five exams (awake anesthesia and

1082　MDCT, MRI using Protocol A, B) are given below the plots. Prediction of

1083　echocardiographic measurements using the cross-sectional modalities was not

1084　possible (P =1).

1085　AoDiam3 (cm): Aortic diameter generated on the three chamber view using the

1086　cross-sectional modalities; LaDiam3 (cm): left atrial diameter measured on three

1087　chamber view using the cross-sectional modalities; PADiam (cm): pulmonary

1088　artery diameter; LaAODiam (cm): left atrium (measured on three chamber view) to

1089　aorta ratio; AoPADiam (cm): aorta to pulmonary artery ratio

1090　AwakeEcho = echocardiogram performed on the awake dogs; DexCT = MDCTA

1091　using anesthetic protocol B; DexMR = MRI using anesthetic protocol B; MidFentCT

1092　= MDCTA using anesthetic protocol A; MidFentMR = MRI using anesthetic protocol

1093　A. Line segments join observations obtained from the same dog as imaging and

1094　anesthesia protocols vary.

1095